RESEARCH ARTICLE OPEN ACCESS

Ultrafast dynamics observation during fem to second laser-material interaction

Nidhi Khobragade, Omkar Nanda Behera,
Gandhi Institute of Excellent Technocrats, Bhubaneswar, India
Capital Engineering College, Bhubaneswar, Odisha, India

ABSTRACT
Femtosecondlasertechnologyhasattractedsignificantattentionfromtheviewpointsoffundamentalandapplication;especiallyfemtosecondlaserprocessingmaterialspresenttheuniquemechanismoflaser-materialinteraction.Undertheextremenonequilibriumconditionsimposedbyfemtosecondlaserirradiation,manyfundamentalquestionsconcerningthephysicaloriginofthematerialremovalprocessremainunanswered.Inthisreview,cutting-edgeultrafastdynamicobservationtechniquesforinvestigatingthefundamentalquestions,includingtime-resolvedpump-probeshadowgraphy,ultrafastcontinuousopticalimaging,andfour-dimensionalultrafastscanningelectronmicroscopy,arecomprehensivelysurveyed.Eachtechniqueisdescribedindepth,beginningwithitsbasicprinciple,followedbyadescriptionofitsrepresentativeapplicationsinlaser-materialinteractionanditsstrengthsandlimitations.Theconsiderationoftemporalandspatialresolutionsandpanoramicmeasurementatdifferentscalesaretwomajorchallenges.Hence,theprospectsfortechnicaladvancementinthisfieldarediscussedfinally.
Keywords:ultrafastdynamics,pump-probeshadowgraphy,ultrafastcontinuousopticalimaging,4Dultrafastscanningelectronmicroscopy,femtosecondlasermanufacturing

INTRODUCTION

Ultrafastlaserscanchangethestatesandpropertiesofmaterials through interactions with them, and they can beused to control the processing of materials from the micro-meter scale down to the nanometer scale or across scales [1].Femtosecond lasers tend to impose extreme conditions intheirinteractionswithtargetmaterialsbecauseoftheultra-shortpulses(approximately10^{-15}s)andultrahighpower intensity(>10^{14} W cm^{-2}) involved, and they can be focusedontonanometerspatialdimensions(approximately10^{-9}m).

Because of the extreme characteristics, femtosecond laserscan be used to process almost any material with high qualityandhighprecisionaswellastoprocesscomplexthree-dimensional structures, which has emerged as a new frontierinthedevelopmentoflasermanufacturingtechnology.Dueto itsnonlinear(e.g.multiphoton)absorption,afemtosecond lasercanovercomethelimitationsoftraditionalprocessing methods; and the accuracy of femtosecond laser fabricationcurrentlystandsat1/50ofthediffractionlimit[2].Thenonequilibrium(e.g.interelectronnonequilibriumandelec-tron-to-latticenonequilibrium) absorptionandnonthermalphasetransitions(e.g.Coulombexplosionandelectrostatic

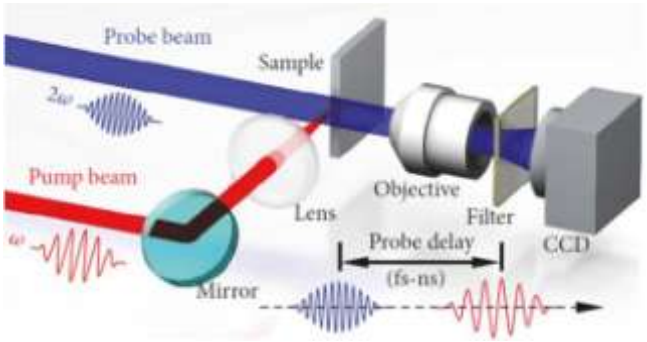

Figure 1.Schematic of the time-resolved pump-probe shadowgraphysetup.Reproducedfrom[30].CCBY4.0

.

stripping) of femtosecond lasers can minimize heat-affectedzones, cracks, and recast layers, thus improving the process-singqualityconsiderably[3,4].Moreover,nomask,vacuum,
or corrosive gas is required in femtosecond laser fabrication.The process generates small quantities of waste compared totraditional methods and does not cause pollution. The char-acteristics of femtosecond lasers have led to the developmentof new manufacturing concepts, mechanisms, methods,
andtechniquesthatsupportalargenumberofmanufacturingapplications in fields such as information technology, bio-technology,pharmaceuticals,aerospace,andenvironmental
industries[5–11].
The mechanism of femtosecond laser fabrication,
including the phase change and material removal, are essen-tially determined by laser-electron interactions [12]. Duringfemtosecond laser fabrication, photons are mainly absorbedby electrons, and the subsequent energy transfer from elec-trons to ions is of the picosecond order. Consequently, latticemotion is negligible within the femtosecond pulse duration,whereas femtosecond photon-electron interactions dominatethe entire fabrication process [12]. Therefore, the regulationof laser-electron interactions or localized transient electrondynamics is critical to the development of femtosecond lasermanufacturing, which makes measurement and control at theelectron level challenging during fabrication processes.
Tounderstandandcontroltheultrafastdynamicprocesses,manyobservationtechniqueshavebeendeveloped.
The pump-probe technique is widely used to capture
theaforementionedultrafastdynamicsthroughrepeatedmea-
surementsandtostudythedynamicprocessesofvarious materials in femtosecond laser manufacturing (section 2). Inadditiontocapturingultrafastphenomenathatareeither
nonrepeatable or difficult to reproduce, many ultrafast con-tinuous optical imaging techniques have been developed inrecent years that can acquire a sequence of temporally andspatially resolved data from a single ultrafast event (section3).Toextractweaksignalsandimprovespatialresolution,four-
dimensionalscanningultrafastelectronmicroscopy
(4D S-UEM) systems have been employed toobservethelocalinstantaneouselectrondynamicsunder
excitation with ultrafast laser pulses. The systems have alsobeen used to reveal the mechanism of the diffusion, migra-tion,ordepletionbehaviorsofsurfacecarriersaswellasthe
influenceofthemechanismontheformationandmodificationofmaterialsandtheenergytransferprocess(section4).Inthefollowing three sections of this review, we comprehensivelysurvey the aforementioned cutting-edge measurement tech-niques.Sometechniqueswereomittedinviewofthelim-
itationonarticlelength.Forexample,ultrafastdetectors,suchas ultrafast framing cameras or steak cameras [13], are notdiscussed. The in-depth description of each technique in thispaper begins with its basic principle, followed by a descrip-tion of its representative applications in femtosecond lasermanufacturing as well as its strengths and limitations. In theconcluding section of this review, a summary and an outlookareprovided.

1. Time-resolvedpump-probeshadowgraphytechniques

Unliketraditionallong-pulselaserfabrication,femtosecondlaserfabricationessentiallychangesthemechanismoflaser-materialinteraction.Currently,manyfundamentalquestionsconcerningtheoriginofthematerialremovalprocessundertheextremenonequilibriumconditionsimposedbyfemtose-
condlaserirradiationremainunanswered.Thisaffectsthequality,accuracy,efficiency,andcontrollabilityoffemtose-
condlaserfabricationandlimitstheextensionoffemtosecondlasermicro-
andnanofabricationtechniquesandapplications.Toacquirelaser-inducedplasmadynamics,severaldiag-nostictechniqueshavebeendeveloped[14–17],amongwhichthetime-resolvedpump-probeshadowgraphytechniquewith micrometerspatialresolutionandfemtosecondtemporalreso-lutionhasbeenwidelyemployed.Inapump-probemethod,apump pulse excites a material, and a second pulse probes thepumped material. By acquiring time-delayed frames, one canreconstructanultrafastmovieofthetime-evolutionreactionofthe material. In particular, shadowgraphy images of transientplasma structures and material ejection provide more infor-mationthantheprobebeamdeflectiontechniquethatcanonlyacquire light intensity refracted by a density disturbance,
andofferinsightsintothermalandnonthermallaserablation
mechanisms [18–22]. Further analysis of the time-

dependentplasmaexpansionandthesubsequentshock waveprocess
according to the point explosion theory can help estimate theenergy conversion, as demonstrated in previous studies forsilicon ablation [23, 24]. In addition, shadowgraphy imagesprovide insights into the plasma dynamics generated underdifferent ablation conditions, such as different thicknesses ofthermallygrownoxidefilms[25,26],airpressures[27],and
excitationofairplasmaathighlaserintensities[28,29].Inthisreview, we focus on the (I) observation of electron densitydynamicsovershapedpulsesand(II) evolutionoflaser-inducedplasmaandshockwaveexpansioncontrolledbyfem-tosecondlaserpulsetrains.

Experimentalsetup
Figure1displaysaschematicofthetime-resolvedpump-probeshadowgraphyexperimentalsetup[30].Thepulsefroma

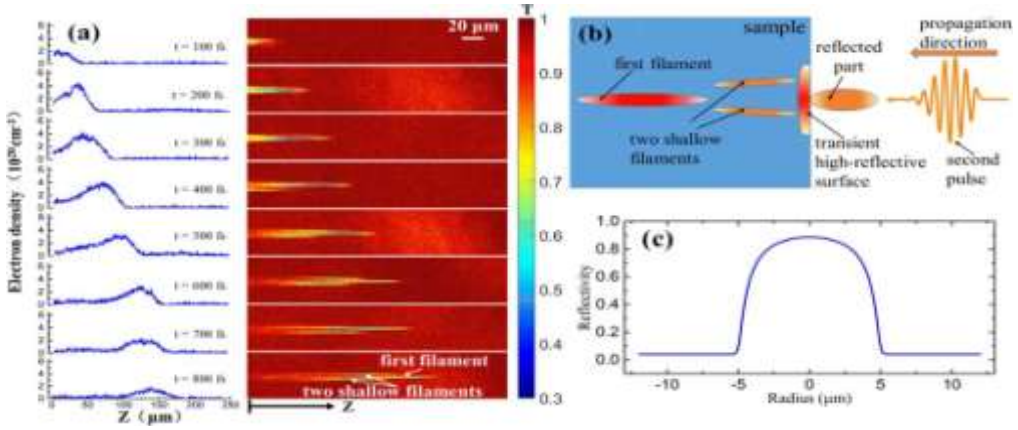

Figure2.(a)Two-dimensionaltransmissionmappingandelectrondensityevolutionatthecentersoffilamentsinducedbydoublepulseswitht_s= 200 fs. The energy of both pulses was 4 μJ. T denotes the transmissivity. (b) Diagram of the filament split caused by the highly reflectivesurfaceinducedbythefirstpulse.(c)Instantaneousreflectivityofthesurfaceatadelayoft=200fsfromsimulation.Reproducedfrom[38].

commercialTi:sapphirefemtosecondlaserwasdividedintotwobeams (pump and probe) with a beam splitter. The pump beamwasfocusednormallyontothesurfaceofsamplematerial.Theprobebeamorientedperpendiculartothepumpbeamwasfre-quency doubled by using a beta barium borate (BBO)crystal
andthenwasusedtoilluminatetheablatedmaterial.Thetransmittedshadowgraphoftheplasmaandtheresultingshockwave were captured by a charge-coupled device (CCD).A400 nm bandpassfilter was placed before the CCD to suppressbackgroundillumination.Anopticaldelaylinewasusedto
controlthe probe delays. To study the dynamics of two-pulseablation, a sequence of shadowgraphs during ablation wasrecorded,withthefirstandthesecondpulsesatdifferentprobedelays.

Observationoftheelectrondensitydynamics overshapedpulses
The femtosecond time-resolved pump-probe shadowgraphytechniqueiseffectivefordetectingtheextremelyfastprocessofelectrondensitydynamicsevolutionunderlaserpulseirradiation. Various aspects of the filaments induced by laserpulseshavebeeninvestigated,suchasthepeakintensity
[31–33],filamentlength[34,35],anddepositionenergy[36,37].However,moststudieshavefocused ontheelectron
dynamics induced by normal Gaussian single pulses. Theresearch on the evolution of electron dynamics induced byshapedpulses(e.g.doublepulsesandmultiplepulses)remains scarce [12]. Electron dynamics depends strongly
onthespatialandtemporalenergydistributionofpulses. Electron density dynamics over the duration of shapedpulsescanbeobservedbyvaryingtheseparationtimeofpulses.Asdisplayedinfigure2,uponthearrivaloftthesecondpulse,filament split was observed. This split was attributed to theemergenceofatransienthigh-reflectivesurfaceinducedbythefirstpulse[38].Thesimulationresultsindicatedthatthereflec-tivityatthecenterofthepulseexceeded0.8,whichcause

dthe secondpulsetobereflectedstrongly.However,intheperic entralarea of the pulse, the reflectivity decreased rapidly. This enabledthe second pulse to enter the sample and induce two shallowfilaments. The experimental results indicated that the energydeposition efficiency can be optimized by shaping the laserpulsestemporally,whichbenefitsthefabricationpr ocess.Afterthe experiments, atomic force microscopy was used to char- acterizetheablationmorphology.

The laser-induced plasma evolution through multipulseablation and the effect of a prepulse-induced crater on thesubsequentlaserfieldwerestudiedusingthetime-resolved pump-probeshadowgraphytechnique[39].Filamentsplitting wasobservedintheearlystagesofplasmaevolution(bef ore ~300fs)(figure3).Thisphenomenonwasattributedtot he competitionbetweenlaserdivergentpropagationinduced bya prepulse-inducedcraterandthenonlinearself-focusingeffect.This was further validated through simulation results. Fila- mentsplittingoccurredintheearlystagesofplasmaevol utionbecause the subsequent laser field was reshaped by the pre-pulse-inducedcrater.

Furthermore,theevolutionoflaser-inducedplasmainfusedsilica has been studied with increasing numbers of pulses.Figure4displaysthetime-resolvedtransmissionoffemtose-cond-laser-inducedplasmawith10–300pulsesat900fs.Asthepulsenumberwasincreased,ah oleformedgraduallywithtwo side branches. The depth of the hole increased, and the sidebranches were formed gradually. When the pulse number washigherthan200,thepeakelectrondensitywassatura ted.Thisbehaviorcanbeattributedtotheinvariabilityof thesidebran-ches.Therefore,thefocusedlaserformedlaser-inducedplasmawiththesamefield,whichensuredthatthe peakelectrondensityapproached a saturation point and did not change. The exper-imental results revealed that energy distribution of subsequentpulses could be influenced by a prepulse-induced structure. Thisis essential for understanding the mechanism of laser-materialinteraction,especiallyinultrafastmultiple-pulselaserablation.

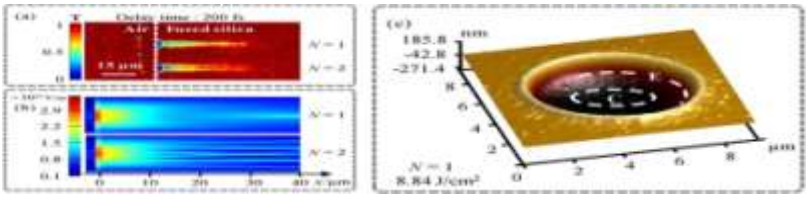

Figure 3.(a) Time-resolved transmission of femtosecond-laser-induced plasma caused by the first pulse (N= 1) and second pulse (N = 2) infusedsilicawithafluenceof8.84Jcm^{-2}at200fs;(b)finite-differencetime-domainsimulationofthelaserfieldconsideringtheKerreffectin fused silicawith the first and secondpulses; and(c) AFM morphology of the crater causedby the first pulse,where 'E' and'C' denote theedgeandthecenterareaofthecrater,respectively.Reproducedwithpermissionfrom[39].©2019OpticalSocietyofA merica.

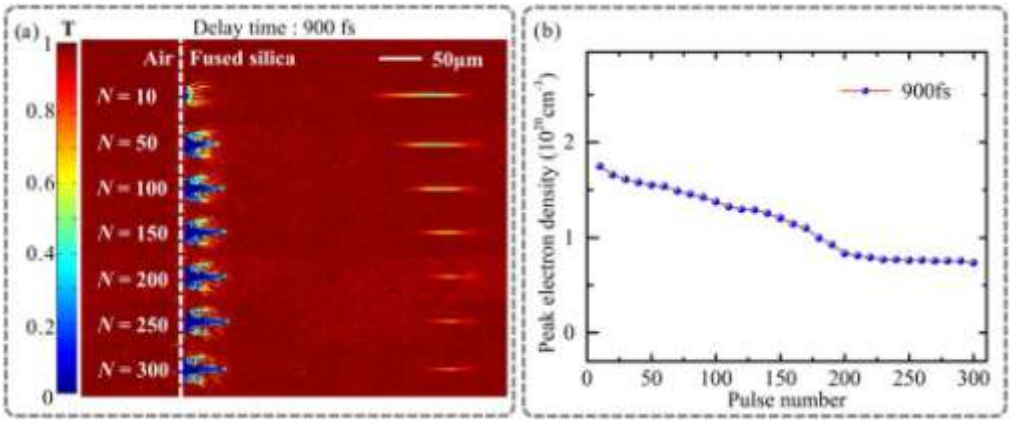

Figure4.(a)Time-resolvedtransmissionoffemtosecond-laser-inducedplasmainfusedsilicawith10–300pulsesand(b)peakelectrondensityevolutionat900fswithafluenceof17.68Jcm^{-2}.Reproducedwithpermissionfrom

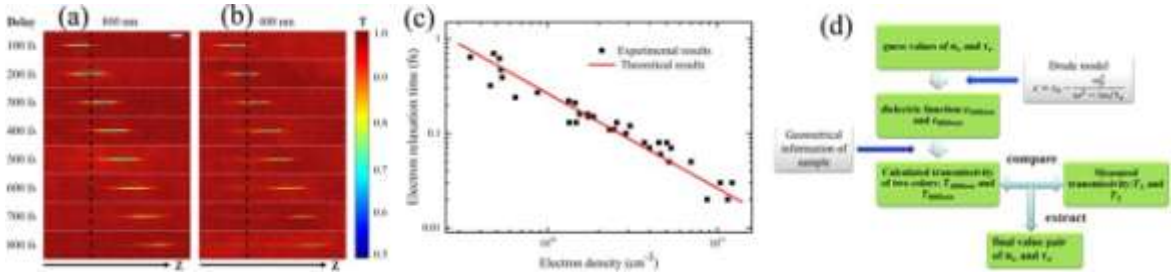

Figure5.Time-resolvedtransmissivitiesofthefemtosecond-laser-inducedregioninfusedsilicawith(a)800nmand(b)400nmprobepulsesatdelaytimesof100–800fs.Thepumppulsesofboth(a)and(b)propagatefromlefttoright.Thecolormapisselectedtoenhancetransmissivitychangesandplasmaevolutionafterlaserpulseirradiation.Thescalebaris20μm.Theblacklineswitharrowsdenotethepropagationdirectionofthepumppulses.(c)Evolutionoftheelectronrelaxationtimewiththeelectrondensity.Theblacksquaresdenotethemeasuredpairsof$n_e$andt_e.Theredsolidlinerepresentsthetheoreticalresultsobtainedusingtheelectron–ionscatteringequation.
(d)Schematicofthemethodfordeterminingthedielectricfunction.Reprintedfrom[45],withthepermissionofAIPPublishing.

The electron relaxation time (τ_e), which is an importantparameter for understanding plasma properties, should be avariable according to theoretical calculations [40–42]. However,inmanyexperimentaltreatments,$\tau_e$hassimplybeen considered a constant [43, 44]. The calculation or measure-ment of $\tau_e$remains challenging. Hence, the spatiotemporalevolution of femtosecond-laser-induced electron plasma infusedsilicawasstudiedusingthedual-frequencypump-probe

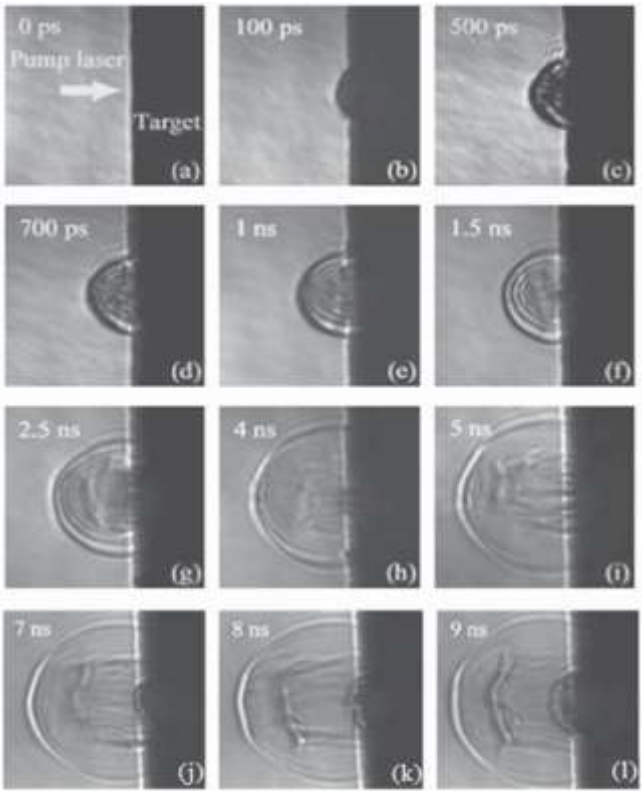

Figure 6.Time-resolved shadowgraphs of material ejection atindicated time delays. Reproduced with permission from [46],Copyright(2007) bytheAmericanPhysicalSociety.

technique [45]. As displayed in figure 5, laser-induced filamentscanpropagateinfusedsilicaforapproximately1 ps,which results in strong absorption of both the 800 and 400 nmprobe pulses. By using the Drude model, a series of transmissivitieswerecalculatedusingmanypairsof$n_e$and$t_e$overa reasonably large scale and with high precision. The calcu-latedtransmissivities and the experimental results revealedthe optimized electron density and the electron relaxation timeof plasma in different parts of the filament at different delaytimes.

Laser-inducedplasmaandshockwaveexpansion

The fundamental mechanisms of ultrafast laser ablation havebeen explained by various theories, such as Coulomb explosion,phaseexplosion,andtheeffectofathermoelasticwave.Ultrafast laser ablation is a composite physical process thatdepends on the laser parameters and the properties of thetarget.Regardingmetaltargets,thedynamicprocessofultrafast laser ablation of aluminum with an energy fluenceconsiderably higher than the ablation threshold was investigatedin[46].Asdisplayedinfigure6,astripepatternprecedingphaseexplosioncanbeobservedintheshadowgraphwithatimedelayof1 ns.Forlongertimedelays, the contrast of the stripe pattern decreases gradually.Intermittentmaterialejectionscanbeobservedwithinthe ejected plumeafter2.5 nsandlongertimedelays.Suchejections have not been observed for semiconductor or dielectricmaterials(e.g.siliconandglasssamples).

Thegenerationoffemtosecond-laser-inducedsurface structures upon the irradiation of multiple pulses is stronglycorrelated with the pulse number, which in turn considerablyaffects successive laser-material interactions. The dynamicsof plasma and shockwave expansion during the ablation offused silica with two femtosecond laser pulses was studiedwith time-resolved shadowgraph imaging [29]. The exper-imental results revealed that during irradiation of the secondpulseonthecraterinducedbythefirstpulse,theexpansionoftheplasmaandshockwave wereenhancedinthelongitudinal direction (figure 7). This enhancement was attributed to thecraterwithconcavelens-likemorphology,whichcanconsiderablyreflectandrefocusthelatterpartofthelaserpulsetoinducestrongairbreakdown(figure8).

A similar enhancement phenomenon was detected in the two-pulseablationofsilicon.Tofurtherverifythefundamentalmechanism, time-resolved shadowgraphy of silicon ablationwasrecordedatthefemtosecondtimescaletodirectlyvisualizethe excitation of air plasma induced by the reflected laser duringthe irradiation of the second pulse [30]. Moreover, the interactionbetweenairplasmaandsiliconplasmawasstudiedatthe picosecond–nanosecond timescale. The study of the interactionindicatedthattheairplasmachannelcanaffecttheexpansion dimension of the plasma and shockwave in the longitudinaldirection; however, the interaction did not affect the morphologyandexpansiondistance(figure9).

Inadditiontothestudiesonfemtosecondtwo-pulse ablation,recentstudieshaveproposedthatthemorphologyofthe laser-induced crater roughens as the pulse number (N)increases [47–50]. This phenomenon leads to a loss of laser-refocusingability,anditcanconsiderablyalterthenatureof expansion of the plasma and shockwave. To study the effectof structure evolution on the dynamics of the plasma andshockwave, time-resolved shadowgraphs were recorded duringablationwithmultiplepulses.Figure10displaysthetypical shadowgraphs of the plasma and shockwave duringablation with the third, fourth, and fifth pulses. Two fundamentalmechanismsofplasmaandshockwaveexpansionwere revealed: the excitation of air plasma and laser-materialcoupling. The two mechanisms were strongly dependent onthe laser-induced surface structure. When the pulse numberwas small, a smooth crater was generated by prior pulses,which could reflect and refocus the next pulse, thus inducingan increased laser intensity above the sample surface. Con-sequently, air plasma was excited and it dominated the anisotropicexpansionofthesiliconplasmaandshockwave.When the number of pulses was large, the smooth craterroughened due to it being covered with microstructures andnanostructures. Consequently, the crater was unable to refo-cus the incident pulse. In this scenario, the air plasma van-ished and laser-material coupling was the core mechanism oftheexpansionofthesiliconplasmaandshockwavewithstrong isotropic characteristics. The findings are of funda-mental importance for obtaining deep insights into the natureofultrafastlaser-materialinteraction.

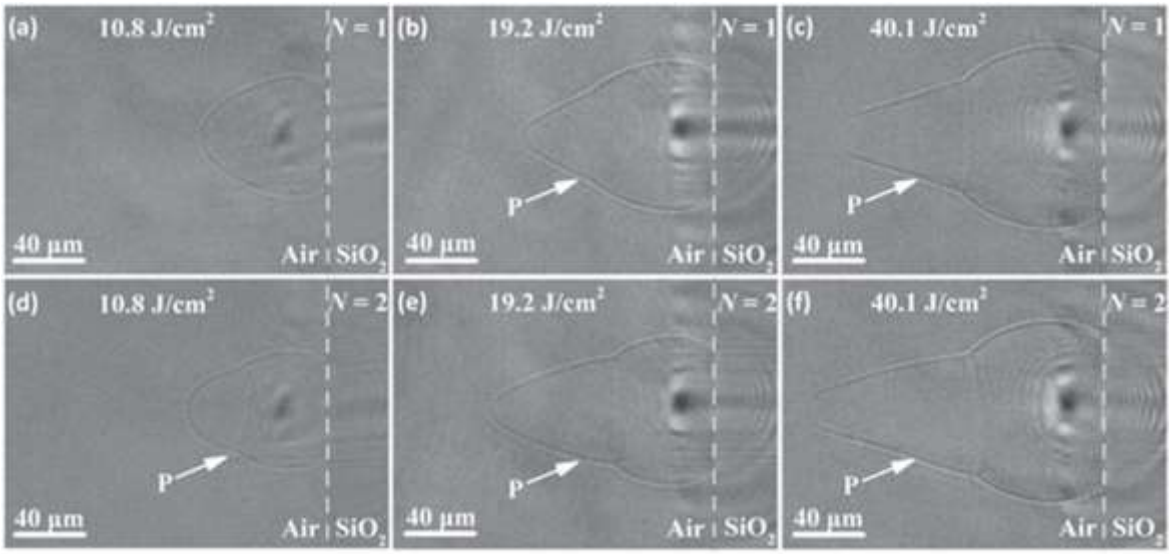

Figure7.Shadowgraphsoftheplasmaandshockwavegeneratedbyfemtosecondlaserirradiationonfusedsilicawithlaserfluencesof10.8,19.2, and 40.1 J cm^{-2}. (a)–(c) Images recorded after the first pulse (N = 1) and (d)–(f) images recorded after the second pulse (N = 2). Pindicates the protuberance on the top of the plasma and the shockwave front. The probe delay was 16 ns. Reproduced with permission from[29].©2017ChinaLaserPress.

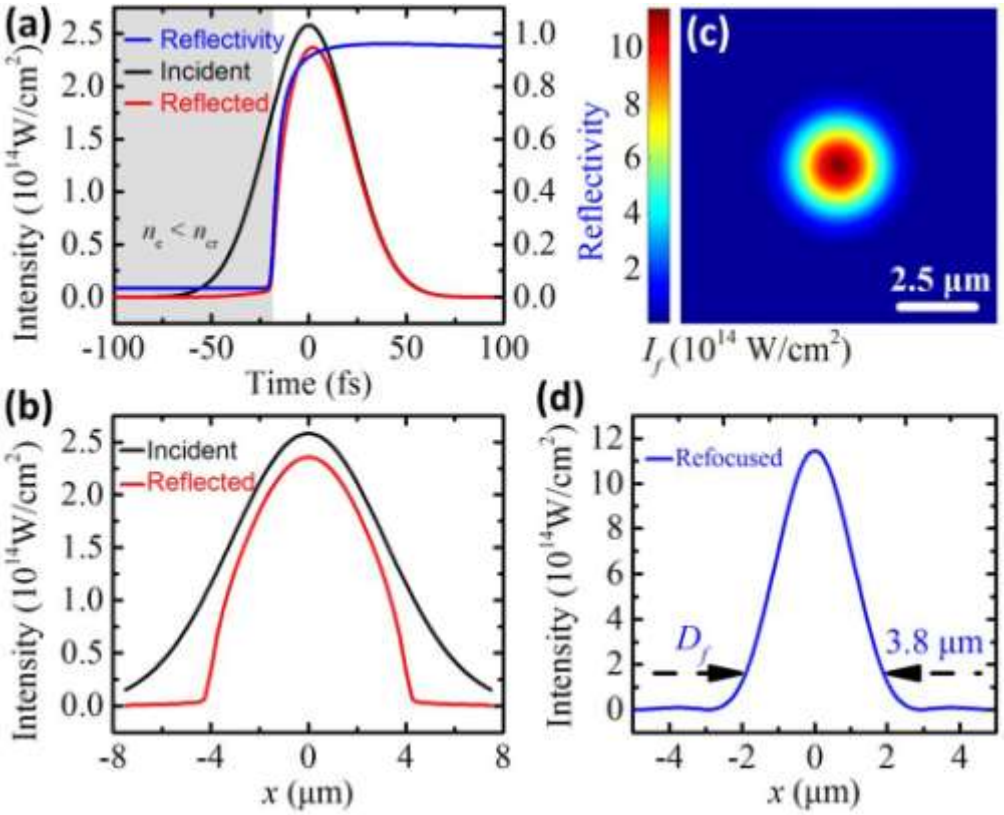

Figure8.Calculationoftherefocusedlaserintensity.(a)Time-dependenceofthesurfacereflectivityandincidentandreflectedlaserintensitiesatthebeamcenter(x=0)duringirradiationofthefirstpulse.(b)Spatialdistributionsoftheincidentandreflectedlaserintensitiesattimezero,atwhichthepeakintensityarrivedduringtheirradiationofthefirstpulse.(c)Refocusedlaserintensitydistributionattherefocusedfocalplaneattimezeroduringtheirradiationofthesecondpulse.(d)Cross-sectionoftherefocusedlaserintensitydistributionattimezero.Theincidentlaserfluencewas13.75Jcm^{-2}.Reproducedwithpermissionfrom[29].©2017ChinaLaserPress.

2. Ultrafastcontinuousopticalimagingtechniques

Pump-probemethodshavebeenimperativeforthestudyofultrafastdynamics.However,theyareinapplicabletomany ultrafast phenomena that are either nonrepeatable or difficultto reproduce, such as chaotic laser dynamics [51], opticalrogue waves [52, 53], light scattering in living tissues [54],andirreversiblecrystallinechemicalreactions[55].Although

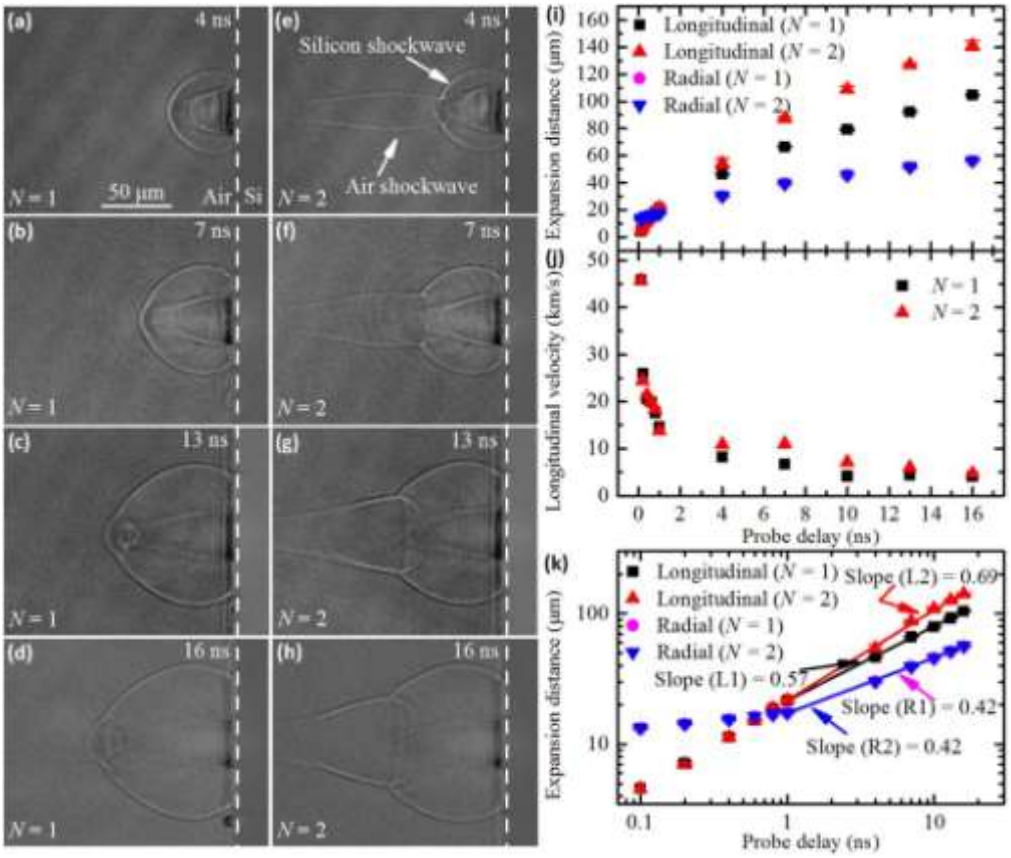

Figure 9.Time-resolved plasma shockwave expansion at probe delays on the nanosecond timescale. (a)–(d) Images recorded for the first pulse.(e)–(h) Images recorded for the second pulse. The dashed line represents the silicon-air interface. (i) Measurements of longitudinal and radialexpansion of the silicon shockwave as a function of time for the first two pulses in the ablation of silicon. (j) Calculated longitudinal velocities ofthe silicon shockwave as a function of time for the first two pulses in the ablation of silicon. (k) Double logarithmic fitting of longitudinal andradialexpansionforthefirsttwopulsesintheablation.Thelaserfluencewas7.27Jcm^{-2}.Reproducedfrom[30].CC BY4.0.

other ultrafast phenomena are reproducible, they have sig-nificantshot-to-shotvariationsandlowoccurrencerates.Examplesinc ludedenseplasmagenerationwithultrafastlasersystems [56, 57] and laser-driven implosion in inertial con-finementfusion[58].Underthesecircumstances,theultrafastcontinuous optical imaging techniques become necessary toovercomethelimitationsofpump-probemethods.Ingeneral,the techniques employ an ultrafast pulse train to record atransientevent.Eachsubpulsein thepulsetrainisassigneda unique optical marker, such as different spatial positions,angles, wavelengths, states of polarization (SOPs), or spatialfrequencies,whichisusedtoseparatethesubpulsestorecover the transient information. In the following subsec-tions,wereviewfourpopularultrafastcontinuousoptical imagingtechniquesbasedondifferentmechanisms.

Ultrafastcontinuousimaging based on spatial division

Themostdirectmethodofcontinuousultrafastimaging involves separating the imaging beams in space,

which is anextensionofMuybridge'simagingsetupforcapturingahorseinmotion[59].Inthismethod,anechelonisusedtoconstruct a probe pulse train, with each subpulse occupying a differentspatial and temporal position (figure 11(a)). Synchronizedwithahigh-speedprocesspassingthroughthefieldofview (FOV),eachsubpulserecordsthetransientinformationoftheprocessatadifferenttime.Theprobesubpulsesareprojectedonto different spatial areas of an image sensor, which thenrecordstheinformationinacontinuousmanner(figure11(b)).

Thistechniqueissuitablefortheobservationofsinglefem-tosecond laser pulse propagation. Because the intense laserpulses develop complex structures during their propagationdue to self-modulation caused by nonlinear effects [60], thepropagation profile is remarkably different from shot to shotevenifthelaserlightsourcefluctuatesmarginally[61].

By using the aforementioned method, high-frame-rateobservation of single femtosecond laser pulse propagation infused silica was realized, which facilitated the determinationof the influence of pulse energy fluctuation on the spatial andtemporal distributions of the single laser pulse [62]. Pump-inducedchangesintherelativereflectivityassmallas0.2% −0.5% were observed in semimetals, which revealed bothelectronicandcoherentphonondynamics[63].

Figure 12(a) illustrates the schematic of the multiframefemtosecond time-resolved optical polarography (M-FTOP)systembasedonechelonspatialdivisionforimagingthe propagationofultrashortpulsesinanopticalnonlinear medium[62].A65 fs,800 nmlaserpulsewassplitintoapump pulse and probe pulse with a beam splitter. The pumppulsewasfocusedatapproximately1mminsideaKerr

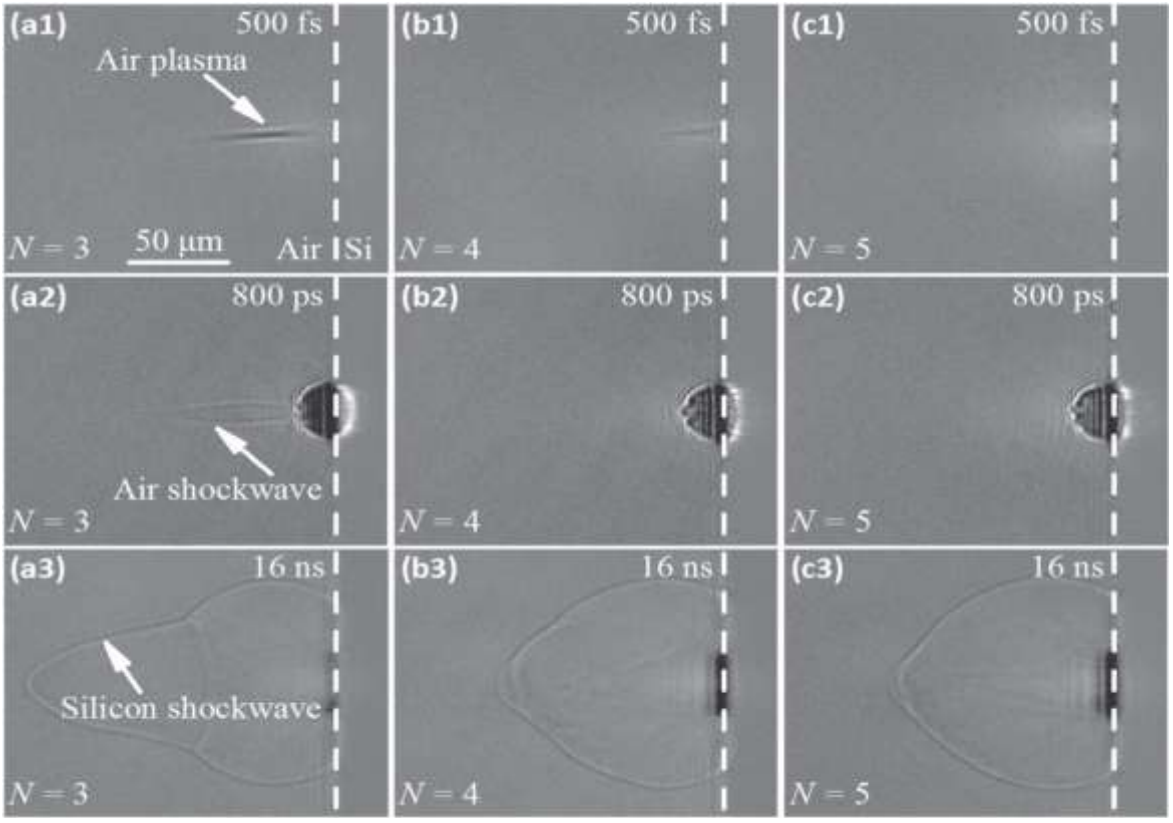

Figure 10 Shadowgraphs of the plasma shockwave at probe delays of 500 fs, 800 ps, and 16 ns during ablation with multiple pulses. (a1)–(a3) Shadowgraphs for the third pulse. (b1)–(b3) Shadowgraphs for the fourth pulse. (c1)–(c3) Shadowgraphs for the fifth pulse. The laserfluencewas7.27Jcm^{-2}.Thedashedlinerepresentsthesilicon-airinterface.Reproducedfrom[30].CCBY4.0.

mediumoffusedsilicaglass(10 mminlength).Thefrequency-doubledprobepulsewasincidentonafour-stepechelonwithastepwidthof0.54mmthatproduceda0.96ps
time delay for the probe pulse. The step height of 0.2 mm
wasconsistentwiththepropagationofthepumppulse.Thepolarizationaxesof thetwo polarizers(P1, P2)placedbeforeandafterthesampleweremutuallyperpendiculartoallowthepassageofpartsoftheprobebeam.Thepolarographyimages
wererecordedwithahigh-spatial-resolutionCCDcamera[64].

Figure 12(b) displays the sequence images in which thespatialresolutionofthepumppulse(45 μJ) propagationdynamicsinfusedsilicawasapproximately 4.3μm.Theframeinterval was approximately 0.96 ps (corresponding to a framerate of approximately 1.05 THz). First, the lateral size of thepumppulsespotchangedmarginally,whichindicatedfilament
generation because of the balance between the Kerr self-focusing and plasma defocusing effects induced by nonlinearionization[65].Specifically,theformationof doublefilamentsduringthepropagationofthepumppulsewasindicatedbytheprofileimagesofthetwopeaks[61].Second,thepulseprofilesvariedfromshottoshotdueto fluctuationsinthepulseenergydistribution,whichhighlightsthenecessityofcontinuousultrafastimaging.Because intensepumppulsepropagationcan leadtothegenerationofcomplexstructuresduetononlineareffects[61],thepropagationprofiledifferssmarkedly frompulseto pulse even if the laser pulse fluctuates only marginally, whichis almost impossible to observe with the pump-probe technique.Thetemporalresolutionoftheimagingsystemcanbeimprovedbyincreasingtheechelonstepwidth; however,itremainslimitedbytheprobepulseduration, whichdependsontheadvancementofattosecondlasers cience[66,67].However,M-FTOPhasafewinsurmountableshortcomings.First,thediscreteprobepulsesaregeneratedbythestepechelon. Hence,theframenumberdeterminedbythestepnumberislimitedbythepowerofa
singlepulse.Moreimportantly,thespatiallydiscreteprobepulsescanonlyimageultrafastdynamicswithnonoverlappingtrajectory.However,observationoftheloca lizedelectrondynamicsinthesameareaisofconsiderableimportanceforresearching
themechanismoflaserfabrication.

Ultrafast continuous imaging based on temporalwavelengthdivision

Recently, a new type of ultrafast continuous imaging methodbasedontemporalwavelengthdivisionwasproposedtoovercometheshortcomingsofthespatialdivisionsystem

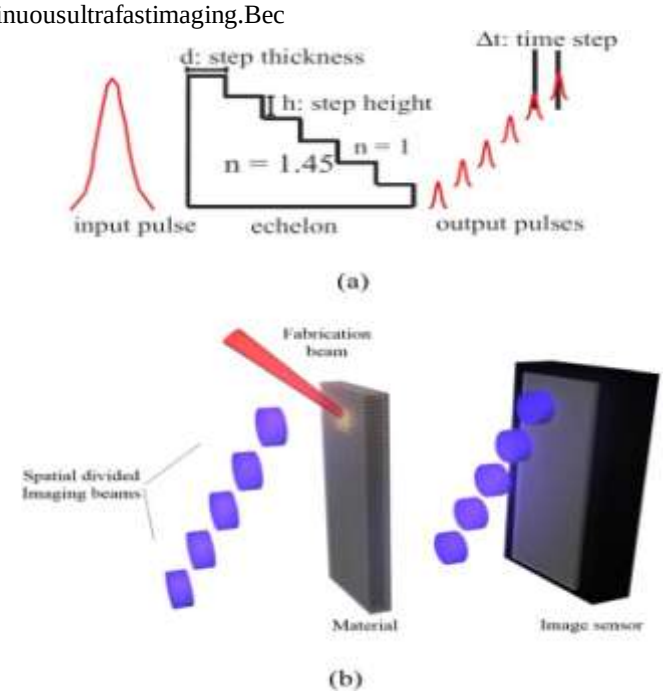

Figure 11.(a)Generationoftime-delayedprobepulsesthroughanechelon.Probebeamspassingthroughthickechelonstepswereretardedrelativetothosepassingthroughthinsteps.(b)Schematic
illustrationofultrafastimagingbasedonspatialdivision.

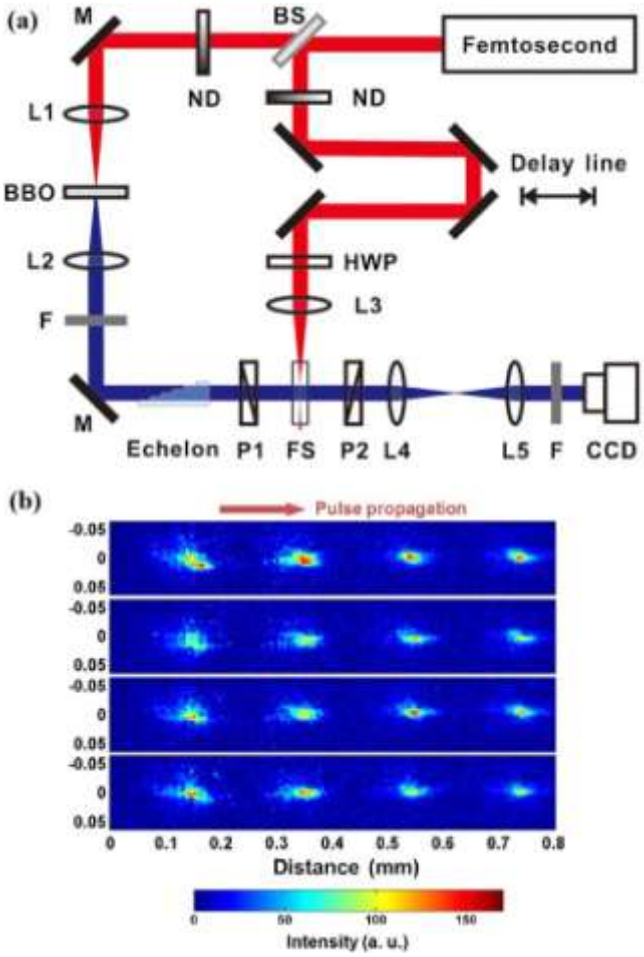

Figure12.(a)SchematicoftheM-FTOPimagingsystembasedon spacedivision.(b)Continuousobservationofdifferentlasershotdynamicsunderthesameconditions.Reproducedwithpermission

[68]. This method employs different wavelengths of indivi-dual pulses to form imaging pulse trains, which are appro-priate for observing electronic dynamic control processing(figure13). The spatial mapping system on thedetection side employsdispersiveopticalelementstospectrallyseparate probepulsesandprojectthemontoanimagesensor.

On the basis of time-stretch imaging [69–71], a repre-sentativetechniqueoftemporalwavelengthdivisioncalled sequentially timed all-optical mapping photography has beendeveloped[72].A70 fsand810 nmpulsewasfirstpassedthrough a temporal mapping device comprised of a pulsestretcher and pulse shaper. Different lengths and dispersingmaterials were used as pulse stretchers to control the chirp ofthe pulse spectrum. Then, a pulse train containing six wave-length-encodedsubpulseswasgeneratedwiththepulseshapert o probe dynamic scenes. The reflected or transmitted signalsubpulses were passed through a spatial mapping unit, whichemployed adiffractiongrating and anarray of periscope mirrors toseparatethesignalsubpulsesinspace(upper-rightinsetin figure 14). Finally, the spatially separated subpulses wererecorded atdifferentareasforeachframeon animagingsensor.

The STAMP system has been applied to visualize early-stagefemtosecond-laser-inducedplasmadynamicswithaframeintervalof15.3ps(correspondingto65.4Gfps)andfrom[62].©2014OpticalSocietyofAmerica.

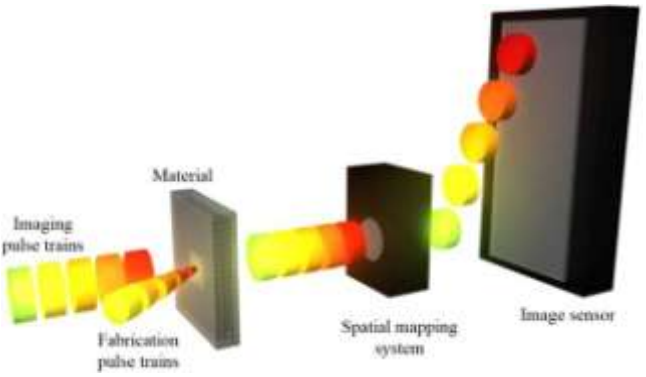

Figure13.Schematicillustrationoftheultrafastimagingmethodbasedontemporalwavelengthdivision.

exposuretimeof13.8 ps(figures14(a) and(b)).Inanexperimentwiththissystem,anablatinglaserpulsewitha pulseenergyof100 μJandpulsedurationof70fswasfocused on the surface of a glass plate. The plasma plumegenerated by the femtosecond laser expanded rapidly alongtheradialdirection,andthespeedoftheplumefrontwas calculatedtobeapproximately$10^5 ms^{-1}$.

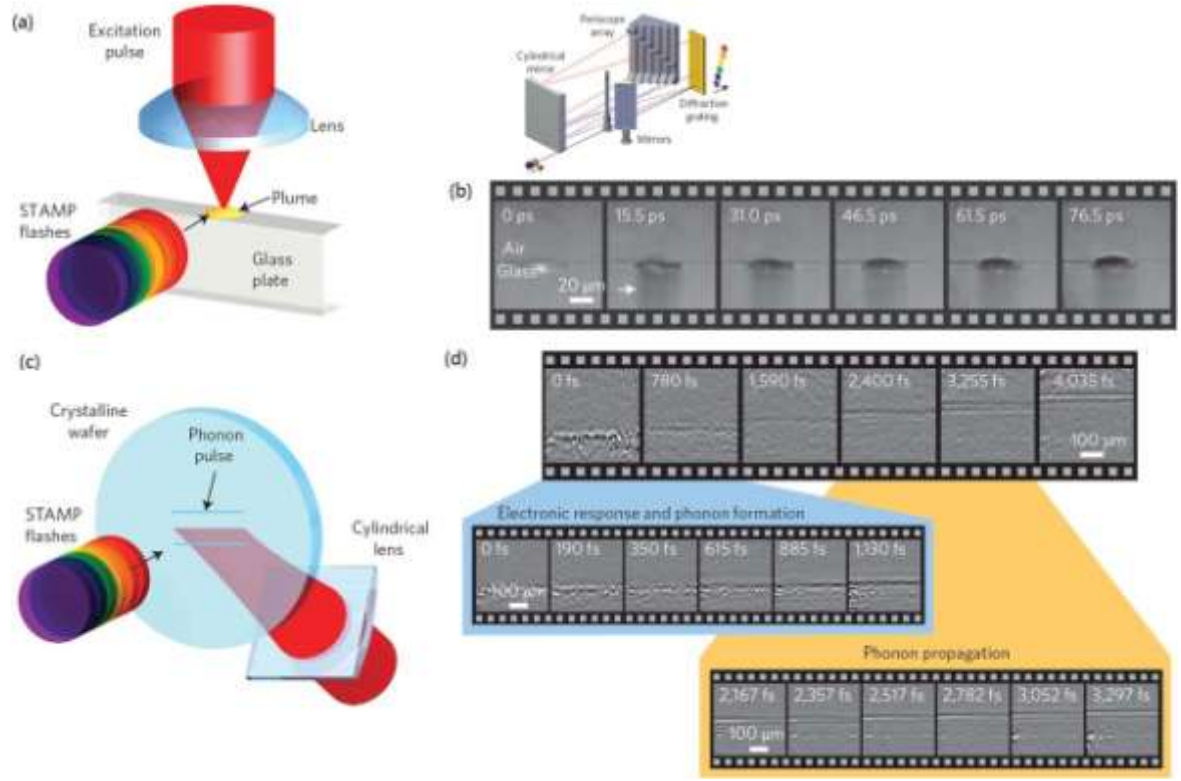

Figure14.STAMP.(a)Schematicofplasmadynamicsobservation.(b)ContinuousimagingofplasmadynamicswithSTAMP.
(c)Schematicofphonondynamicsobservation.(d)ContinuousimagingofphonondynamicswithSTAMP.Inset:Aspatialmappingunitemployingadiffractiongratingandanarrayofperiscopemirrorstoseparatepulsetrainsinspace.Reprintedbypermissionfrom Macmillan PublishersLtd:NaturePhotonics[72],Copyright2014.

Moreover, STAMP has been used to observe phonondynamics at the femtosecond time scale (figures 14(c) and (d)).An excitation pulse (pulse energy: 40 μJ) was line-focused ontoa ferroelectric crystal ($LiNbO_3$) wafer at room temperature toproduceacoherent phonon-polaritonpulse through impulsive
stimulatedRamanscattering.Thephononpulseformation wascapturedwithaframeintervalof812fs(corresponding to1.23Tfps) and exposure time of 1020 fs. Frames from a STAMPmovie of the phonon dynamics are displayed in figure 14(d).Theframesillustratetheentiredynamicprocess,including the
generationoflaser-pulse-
excitedlatticevibrationsinthecrystalandthepropagation ofaphonon-polaritonwavepacket.In
addition, figure 14(d) depicts the propagation of a wave packetwith a frame interval of 229 fs (corresponding to 4.37 Tfps).Thespeedofthephonon-polaritonwavepacketwascalculatedfrom the acquired images to be 4.6×10^7 m s^{-1} (one-sixth ofthe speed of light). However, the total number of frames in asingleshotofthissystemwaslimitedtosixduetothesimple
embodimentofthespatialmappingsystem.
Subsequently,severalsimilartechniqueshavebeendeveloped toreducethecomplexityandimprovetheperformanceoftheSTAMPsystem[73–
76].Forexample,thepolarizationstatecanbeusedasan opticalmarkercombinedwiththewavelengthmarkerto improvethespatialmappingsystem[73,76].Aspectrallyfiltered(SF)-STAMPsystemwasdeveloped with a different spatial mapping method [74, 75]. AschematicoftheSF-
STAMPsystem[74]isillustratedinfigure15(a).Thissystemexpandedtheprobelaserbandwidth
from 20 to approximately 40 nm and eliminated the requirementfor the pulse shaper used in the temporal mapping device.Instead, the system was equipped with a frequency-chirpedpulsetocaptureultrafastevents.Thespatialmappingdevice
was replaced with a diffractive optical element (DOE) and atiltedbandpassfilter [77,78].TheDOEcangenerate25spa-
tially resolved replicas of the signal pulse, which are incident onthe bandpass filter at different angles. Hence, different trans-
missivewavelengthscanbeselectedaccordingtotheincidentanglestoformtheimagingsequence[77].Thesequencedepthcan be determined according to the number of replicas producedby the DOE. The temporal resolution of imaging can be con-trolled through spectral dispersion; however, the resolution islimitedbythetransmissivewavelengthrange.Anobservation
timescalefromsubpicoseconds(approximately10^{-13}s)tosubnanoseconds(approximately 10^{-10} s) can be achieved [75].TheSF-STAMPsystemwasappliedtocapturethe
dynamics of the crystalline-to-amorphous phase transition ofthe $Ge_2Sb_2Te_5$ alloy induced by a frequency-doubled
pumppulse.Thegradualchangesintheimagesof25frames(figure15(b))withanaverageframeintervalof133fs
(correspondingto7.52Tfps)indicated
thefollowing:the
amorphizedareahaddecreasedreflectance,andthephase
change domain did not spread spatially to the surroundingcrystalline area. These findings experimentally verified thetheoreticalphasetransitionmodelthatattributedtheinitiationofnonthermalamorphizationtothedisplacementofgerma-
nium(Ge)atomsfromoctahedraltotetrahedralsites[74,79].

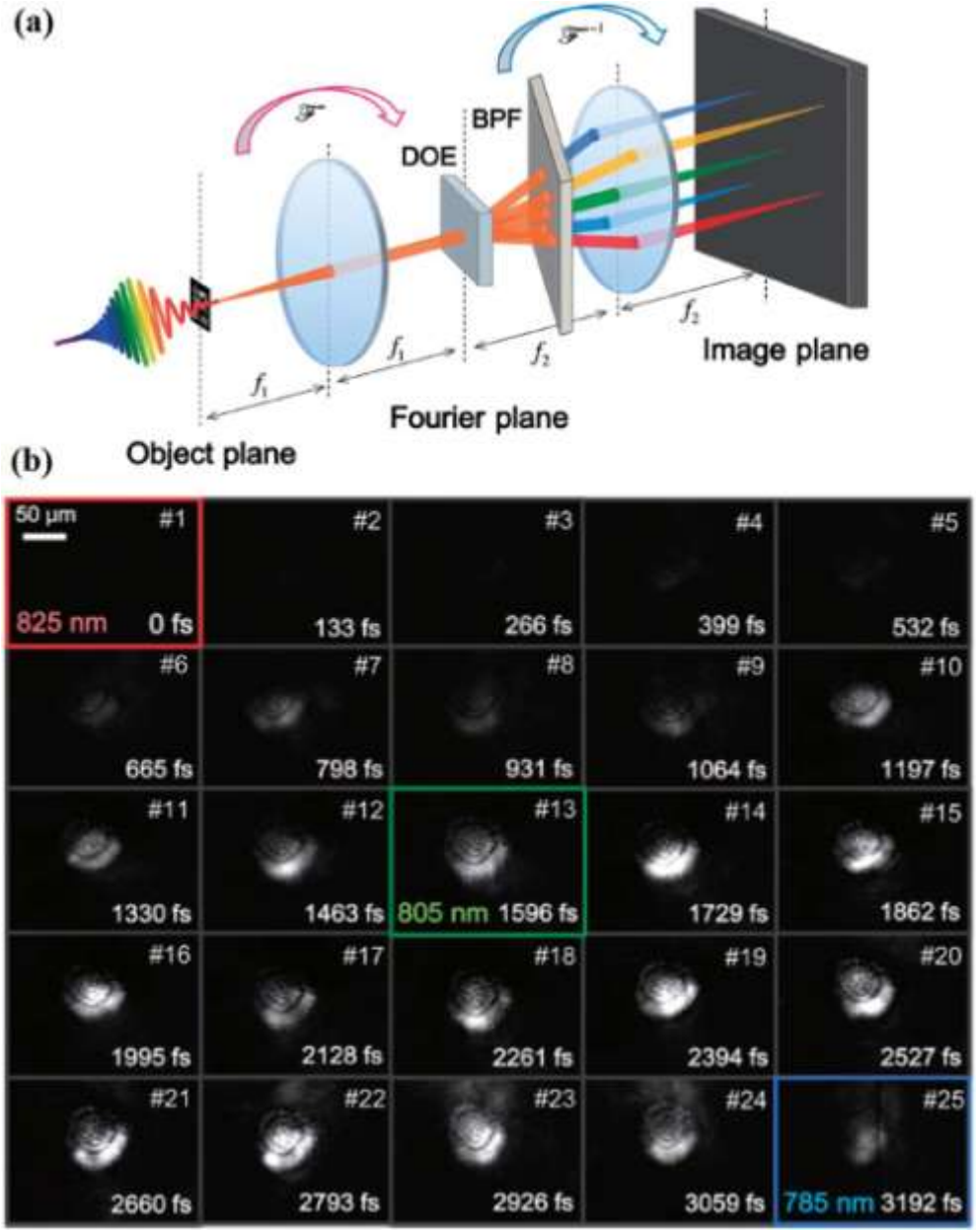

Figure 15.(a) Schematic setup of the spectrally filtered (SF)-STAMP system and (b) sequence images of the crystalline-to-amorphous phasetransition of the $Ge_2Sb_2Te_5$ alloy captured by the 25-frame SF-STAMP at 7.52 Tfps. Reproduced from [74]. © IOP Publishing Ltd. CC BY3.0.

Continuous imaging of light propagation at a frame rateof3.85Tfpsfor60frameswasachievedbycombining temporal wavelength division with the compressed sensingalgorithm.Thistechniqueiscalledcompressed ultrafast spectral-temporal(CUST) photography[80].Inthisima-gingsystem,an800 nm,50 fslaserpulse (bandwidth:18 nm) is stretched with a grating pair. By tuning the incidentangleofthegratingpair,thetemporalresolutionofthe system can be tuned continuously from 0.1 to 5 ps. On thescene plane, the stretched pulse is transmitted through anultrafastobjectandthenprojectedontoadigitalmicro-mirrordevice(DMD).TheDMDspatiallyencodesthesignal pulse with pseudorandom binary patterns. The encodedpulseisfurtherdispersedusingasetofopticsand d

received onto a CCD sensor. Multiple temporally or spec-trallyresolvedimagescanbereconstructedfromtheres ulting compressed two-dimensional image by using thecompressedsensingalgorithm.
The frame number (60 frames) and imaging speed (7.52Tfps) of the CUST photography system and the SF-STAMPtechnique,respectively,areamongthehighest intheultrafast optical imaging domain. Although the light throughput of theoriginal STAMP system is high, the system is limited by alowsequence depth.Bycontrast,theCUSTphotographysystemandt heSF-STAMPtechniquehaveincreasedsequence depth at the cost of a considerable decrease in lightthroughput. In addition, these techniques are applicable onlytoultrafastprocessesinsensitivetothewavelength .

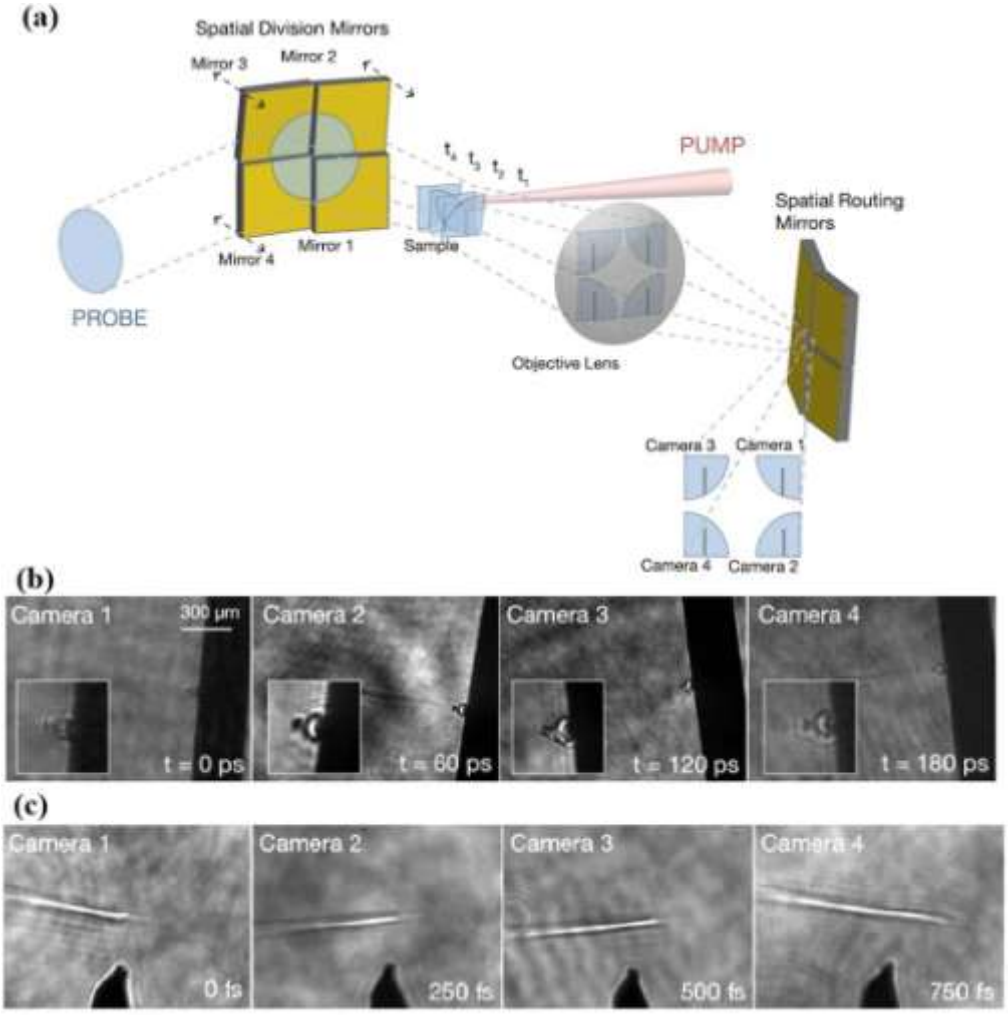

Figure 16.(a) Schematic of the ADMC system. The incoming probe pulse is projected onto a two-by-two mirror array that splits the probeinto four sub-beams with different temporal delays. Another set of two-by-two mirror arrays is used to route the sub-beams to individualcameras. (b) Four frames of femtosecond-laser-induced plasma creation and ablation on the surface of a metal wire. (c) Four frames of afemtosecond-laser-inducedionization frontpropagating inair. Reproducedwith permissionfrom [81].©2018Optical Societyof America.

Ultrafastcontinuousimaging based on angledivision
Intheangle-
divisionmethod,atransienteventisprobedfromdifferent angles to avoid the spectral problems of STAMP orCUST. For example, an angle-division-based multiple-
camera(ADMC)systemwasdevelopedwithtwosetsoftwo-by-two
mirrorarrayswithdifferentanglesforspatialandtemporal
division and routing of multiple probe pulses [81]. This sin-gle-shot scheme (figure 16(a)) was successfully applied tocapturefemtosecondionizationfrontspropagatingat the
speed of light in air as well as laser-induced ablation of solidtargets (figure 16(b)). The ADMC system was developed toprovide individually adjustable frame intervals ranging from30fstohundredsofpicoseconds.
As depicted in figure 16(a), an 800 nm, 30 fs pulse is splitinto a pump pulse and probe pulse. The frequency-
doubledprobepulseforimagingisspatiallysplitintofourbeamswith
atwo-by-twosquare-
mirrorarray.Eachmirrorisangledmarginallyinwardsothatallbeamscrossthetargetlocatedata designed position from the mirror array. Moreover, eachmirrorissetonitsowntranslationstagesothatthetemporal
delay of each beam can be adjusted individually. After pas-singthetargetplane,thefourprobebeamsarereflectedindependently by another two-by-two square-mirror array,whichisangledoutward,anddirectedtowardindividualcamerasthroughasingleimaginglens.
Thedynamicsoflaser-
inducedplasmacreationandexpansionarecapturedatthetimescalesofhundredsoffemtosecondstopicoseconds.Figure16(b)displaysfour
successiveframes of femtosecond-laser-induced plasma
creation and ablation on the surface of a metal wire. Theframeswerecapturedat0,60,120,and180ps.Atapproxi-
mately4 psbeforethearrivalofthepumppulse(t = 0), aplasmaplumewithahemisphericalshockboundarywas
formed on the surface (Camera 1). The formation of thisplume was attributed to a pump pulse that arrived 10 ns beforethemainpumppulse.Thearrivalofthispumppuleisevi-
dent from the absence of an air ionization trail in the imagecaptured by Camera 1; but the presence of an air ionizationtrailisseenintheimagescapturedbyCameras2,3,and4.Inaddition,thesizeoftheplasmaplumeandtheshock

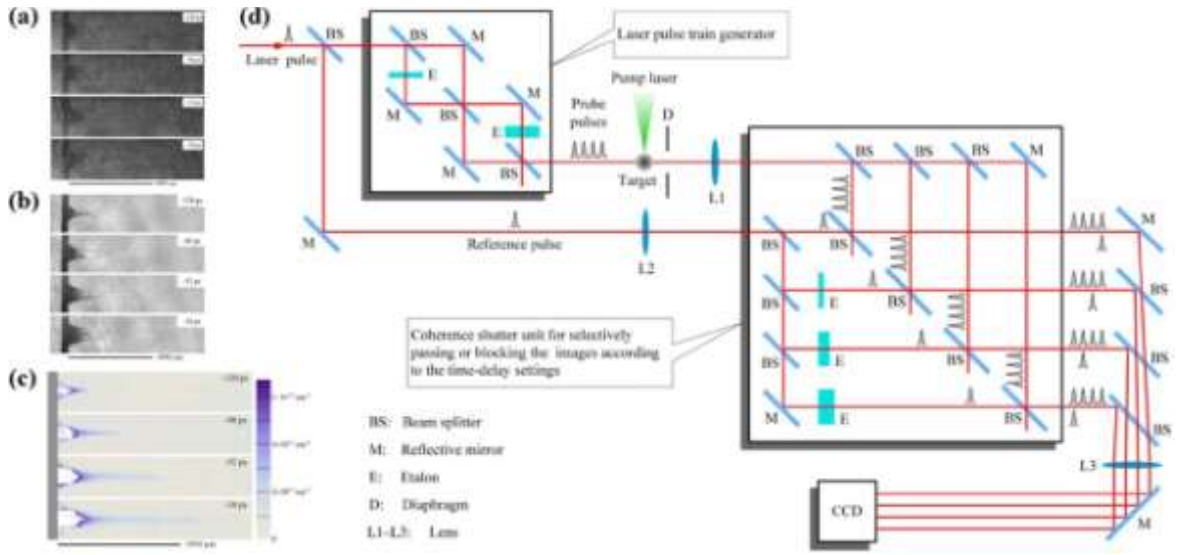

Figure17.Formationofthedischargepathgeneratedbyirradiatingaluminumfoilwithalaserhavingapumplaserenergyof 108mJ.
(a)Fourhologramsobtainedat−120,−86,−52,and−18ps;(b)reconstructedlightintensityimages;(c)reconstructedelectronaredensityimages;and(d)
layoutoftheOCFIsystem.Reproducedwithpermissionfrom[82].©2017OpticalSocietyofAmerica.

boundary did not change after 180 ps, which indicated that theplasma expanded over a considerably longer time scale, suchas nanoseconds. At t = 60 ps, the main pump pulse interactedwith the target surface and formed a smaller plasma. Similartothelargerplasma,thesmallerplasmadidnotchangeconsiderably over a few hundreds of picoseconds. This dou-ble plasma formation is a rare event and does not alwaysoccurinrepeatedexperiments,whichindicatestheusefulnessof continuous imaging diagnostics when capturing unusualultrafast events. In addition, sequences of a femtosecond-laser-inducedionizationfrontpropagatinginairwerecaptured withatemporalresolutionof250fs(figure16(c)).

Anothermethodofangledivisioninvolvesextracting informationatdifferenttimesfrominterferometricimagescaptured atdifferentangles.Here,weintroducetworepresentativeworks. One is the all-optical coaxial frame imaging (OCFI)methodbasedonparallelcoherenceshutters,inwhichatrainof laserpulsescoaxiallyilluminatesthetargetandgeneratesholo-grams in different areas in the spatial domain [82]. With theOCFImethod,nonmultiplexingserialimageshaving hightemporalandspatialresolutionwithidenticalspatial,temporal,andchromaticbenchmarkscanbecapturedinasingle shot (figure 17). As displayed in figures 17(d), (a) 527 nm, 10 pspulseissplitintoaprobepulseandreferencepulse.The probe pulseissplitintoatrainoffourcoaxialdaughterpulseswithatemporalintervalof 34 ps with three beam splitters and twoetalons.Thepulseenergyofeachdaughterprobepulseatthe target is approximately 0.1–1 μJ. After passing through thetarget,thepulsetrainissplitintofouridenticalpulsetrains, whereasthereferencepulseissplitintofourpulseswithdifferenttimedelays.Thetimedelayofaspecificreferencepulseissettobe the same as that of a specific daughter probe pulse so thateachprobepulsetrainonlyinterfereswithaspecificreferencepulseandgeneratesauniquehologram.Then,thefourspatiallyseparated holograms are projected onto four nonoverlapping areasinaCCD.Eachhologramisseparatedspatiallyandtemporallyfromtheothersbyusingacoherenceshutterwithouttheassistanceofanymechanicaloroptoelectronic device.

A1064nm,150ps,and100mJpumppulsewasfocusedona 70 μm thick aluminum foil. Pump-laser-induced 'superfast jets'were ejected from the ablation side (figures 17(a)–(c)), whichmaybeconsideredadischargepath.Theapparentvelocityofthe 'jet' front exceeded 9000 km s^{-1}. The 'jet' tail mainly consistedofdenseplasmathatblockedtheprobelaseranddappearedasashadowintheholograms.Thelightintensityimages(figure17(b))and theelectron densitymaps(figure17(c))related tothelightphasewerereconstructedfromtheholograms (figure 17(a)). The maximum electron areal density and max-imum electron volume density of the 'jet' head were approximately$2\times10^{17}cm^{-2}$and$1\times10^{20}cm^{-3}$,respectively.

Figure18(a) illustratesanotherangle-divisionsystemcalledsingle-shotfrequency-domaintomography(SFDT)for reconstructingultrafast spatiotemporaldynamics[83].Inthis technique, an 800 nm, 30 fs pump pulse creates an evolvingluminal-velocity refractive index structure in a fused silicaglass due to its nonlinear refractive index and the pump-generatedplasma.Athree-layerstructureconsistingofaBBOcrystalsandwichedbetweentwoHZF4glassplateswas employedtogenerate15frequency-doubledprobepulsesfrom a pair of spatiotemporally cross-incident pulses (800 nm,30 fs, 30 μJ). Among the 15 probe pulses, five probe pulseswithdifferentprojectionangleswereselectedandoverlapped both spatially and temporally at the target for continuousimaging of a transient, which was measured using spectralimaginginterferometry[84–86].Thereferencepulserecordedthephasereferenceandtheprobepulsesthatinterferedinside the spectrometer and projected a grid-like frequency-domainintensity pattern or hologram onto a CCD camera [87]. Theevolutionimageswerereconstructedbywindowingandinverse-Fourier-transformingthehologramareaassociatedwith each probe pulse and applying the tomographic imagereconstructionalgorithm[83,88].

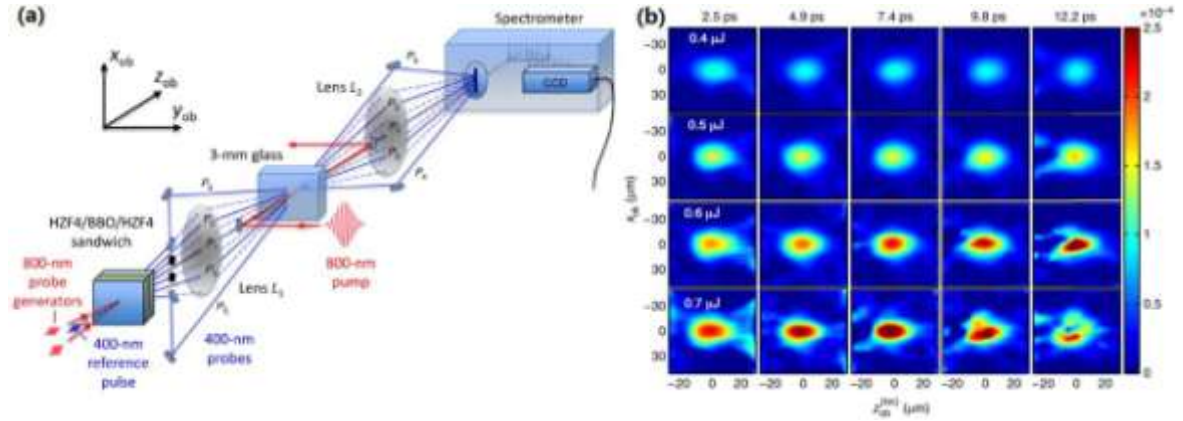

Figure18.(a)SchematicoftheSFDTsystembasedonangledivision.(b)Imagingofthenonlinearindexprofileatfourdifferentpumpenergiesandfivedifferentpropagationtimes.ReprintedbypermissionfromMacmillanPublishersLtd:NatureCommuncations[83],Copyright2014.

Figure 18(b) displays frames from SFDT movies of theevolvingindexprofileinducedbythepropagationofan ultrafastlaserpulseinafusedsilicaglasswithdifferentpulseenergies. The temporal resolution of the reconstructed

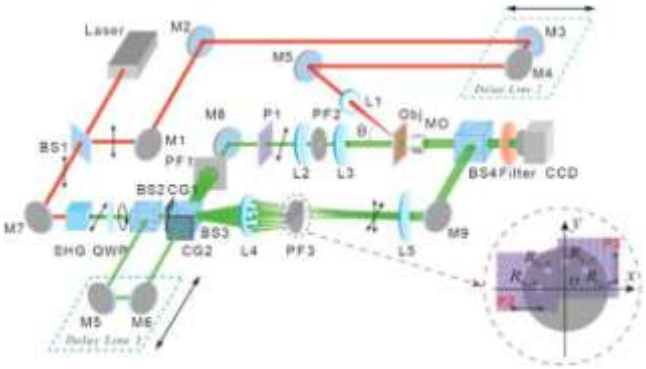

Figure19.SchematicoftheTHPMexperimentalsetupforimaginglaser-induceddamage.Theblackarrowsindicatethepulses'SOPs.Lower-rightinset:generationoffourreferencepulseshavingdifferentspatialfrequencies.Reproducedwithpermissionfrom[90].

moviewasapproximately2.5 ps.Thereconstructedmovierevealedaseriesofnonlinear dynamics,especiallyathighpulseenergies,suchasself-focusingofthepulsewithin7.4psandtheformationofaspatiallobeduetolaserfilamentationat 9.8 ps.Inaddition,theindex'hole' displayedinthefinalimageat12.2psindicatesthattheplasmageneratedinduceda negative index change that locally offset the laser-inducedpositivenonlinearrefractiveindexchange.

The interferometry imaging method can record complexamplitudes and capture dynamic events along the propagationdirections of probe pulses. However, the limited number ofillumination angles results in artifacts that strongly affect thereconstructedimages[89].Consequently,thespatialresolutionofthismethodissuitableforimagingsimplestructuredobjectsonly.

Ultrafast continuous imaging based on spatial frequencydivision

Thelastmethodintheultrafastcontinuousimagingdomainisspatialfrequencydivision,whichaddsdifferentspatialcarrier

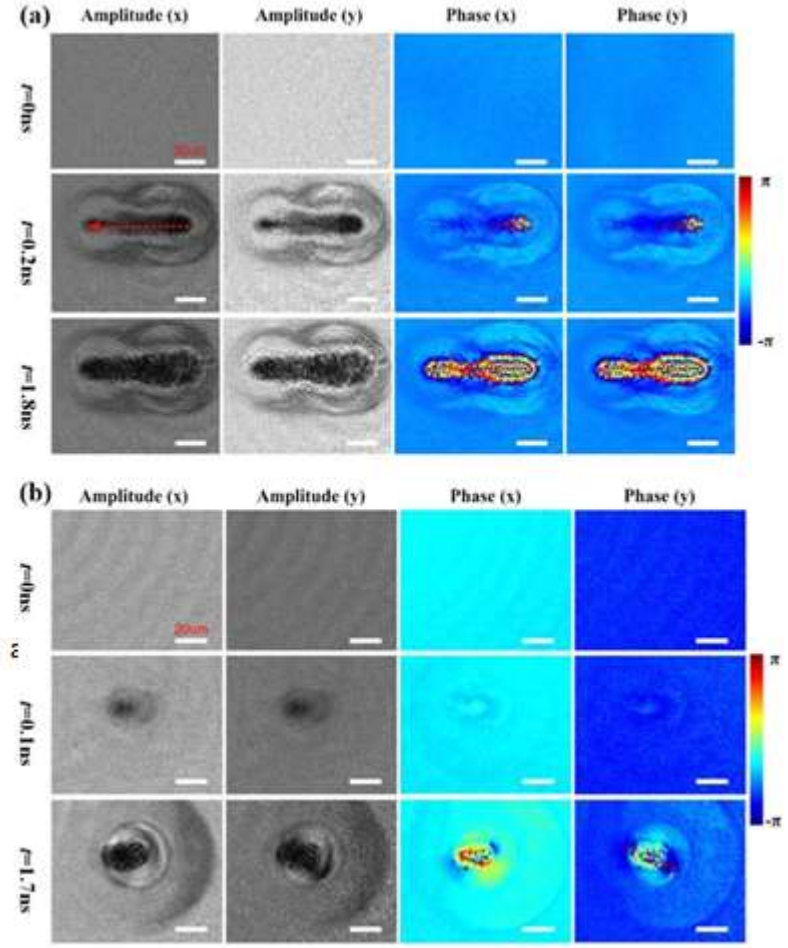

Figure20.Time-resolvedamplitudeandphasecontrastimagesofultrafast-laser-induceddamageina(a)linearpolarizerand(b)micalaminasample.Reproducedwithpermissionfrom[90].©2017OpticalSocietyofAmerica.

frequencies to different probe pulses. Through image reconstruction,spatiallysuperimposedtemporalinformationcanbeseparated in the spatial frequency domain to realize ultrafastcontinuous imaging. Two representative techniques are discussedinthefollowingtext.

Figure 19displays the time-resolved holographic polar-ization microscopy (THPM) system based on spatial frequencydivision for monitoring laser-induced ultrafast phenomena inpolarization-sensitivematerials[90].A1064nm,30psimaging probe pulse was frequency doubled, tuned to circular polarization,andthensplitintotwopulseswithatimedelay.Each

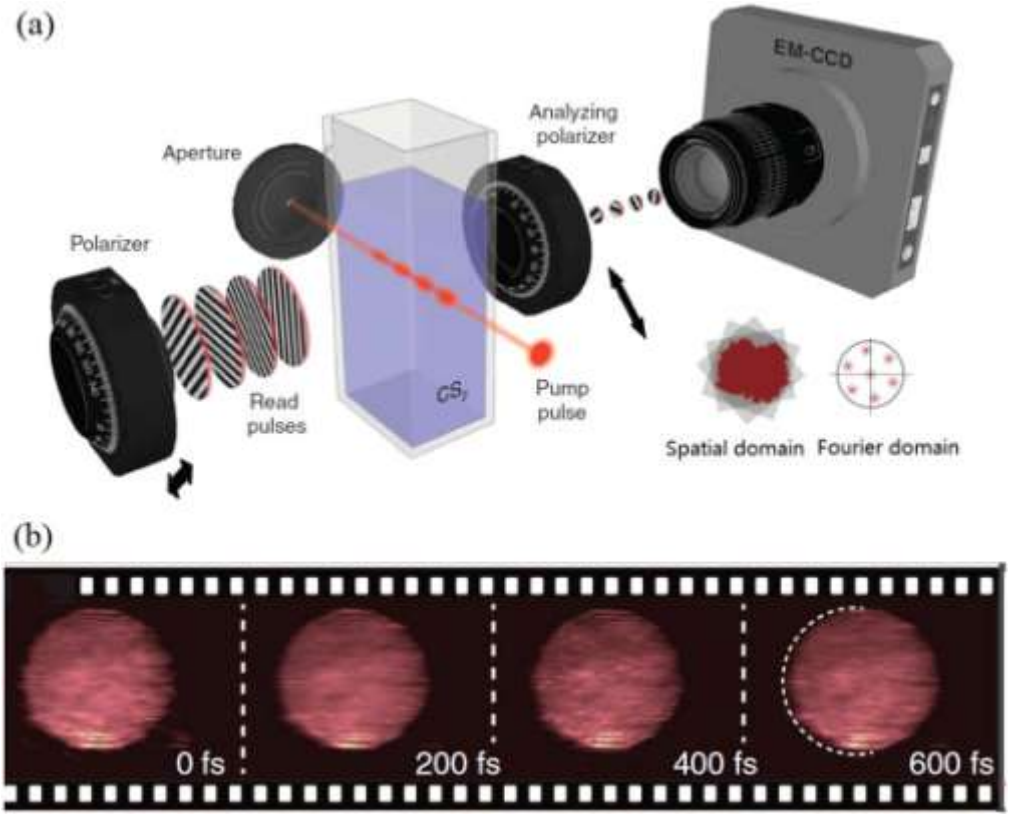

Figure21.(a)SystemschematicoftheFRAMEimagingbasedonspatialfrequencydivision.(b)SequenceofreconstructedframesofapropagatingfemtosecondlaserpulseinCS_2liquid.Reproducedfrom[95].CCBY4.0.

probe pulse was further split into signal pulses and referencepulseswithdifferentSOPs.Hence,twosignal pulsesandtworeference pulses were generated and further passed throughdifferent spatial filters to load different spatial carrier frequencies.Then,theinterferencehologramsofthesignalpulsesand reference pulses with different spatial frequencies
wererecordedwithaCCDcamera.Finally,theamplitudeandphaseinformationoftwoorthogonalpolarizationcomponentsoftwosequentialvectorwavefrontswithultrashorttimeintervalswereretrievedbyperformingimagereconstruction[91].

THPM was applied to the real-time imaging of laser-induced damage (figure 20). A thin film linear polarizer wasobservedwithapumpenergyfluenceof1.1 $\times 10^2$ J cm^{-2}(figure 20(a)). The amplitude and phase distributions of twoorthogonalpolarizationstatesoftheobjectwavesassociated
with two different time delays of 0.2 and 1.8 ns were obtainedsimultaneously at an imaging speed of 625 Gfps. The distributionsindicatedthattherelativeindexchangebetweenthetwo orthogonal polarization states was nearly identical in theprocessoflaserirradiation.Inaddition,amicalaminaplatewas
testedwithapumpintensityof>40Jcm^{-2}(figure20(b)).The initialamplitudeandphasechangecapturedby thesystemat
0.1 and 1.7 ns verified the generation and propagation of shockwaves and revealed nonuniform changes in the
transmissionandrefractiveindicesintheprocessoflaserirradiationbecauseofthesample'sanisotropy.

Thetime-resolvedpolarizationimagingtechniqueisimperativeforinvestigatingtheultrafastphenomenainpolarization-sensitivematerialsbecausefocusedfemtosecondlaser irradiation in isotropic materials, such as fused silica[92, 93], induces artificial birefringence modification. TheTHPM system with an improved temporal resolution can beapplied to study other ultrafast events, such as free-electrongenerationandlatticeheating[94].

Anothertechniquebased on spatial frequencydivision is
frequencyrecognitionalgorithmformultipleexposures(FRAME) imaging [95]. Instead of forming the interferencefringes,FRAMEencodesvariouscarrierfrequenciestoprobesubpulsesthroughintensitymodulationachievedwithaRonchigrating.Byusingthissystem,a 125 fsprobepulsewas split into four subpulses. The intensity profile of eachsubpulse with a specified time delay was modulated usingRonchi gratings with an identical period but unique orienta-tions

(figure 21(a)). Thus, the dynamic temporal informationofthescenecouldbecapturedwithaCCDcamerainasingle shot and separated in the spatial frequency domain withoutanycrosstalk.Finally,theimagesequencecouldberecoveredthrough image reconstruction according to the THPM technique.ByusingtheFRAMEimagingsystem,thepropagation of a femtosecond laser pulse through carbon disulfide (CS_2)liquid was captured with a temporal resolution of 200 fs(corresponding to animagingspeed of5Tfps)(figure21(b)).

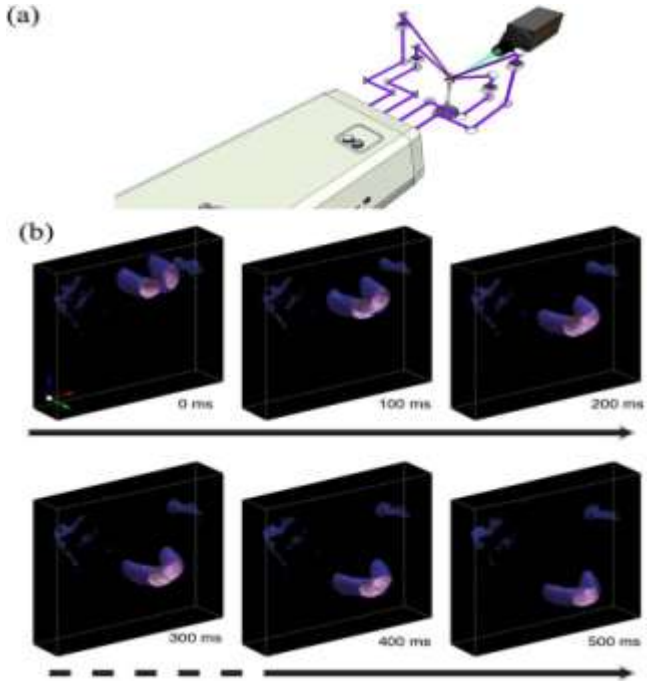

Figure22.(a)Opticalarrangementforthespectroscopicandlasersheetexperimentsconductedusing FRAME.(b)Temporallyresolved3DimagingusingFRAMEcombinedwithlasersheet illumination.Therecorded3Dsequencedisplaysadyedropletfallingthroughacuvettewithwater.Reproducedfrom[95]. CCBY4.0.

Because each FRAME image is extracted using a uniquespatial code, the method does not rely on a specific opticalwavelength or laser bandwidth. Therefore, it can be used forspectroscopicmeasurementsor3Dimagingcombinedwith lasersheetillumination(figure22).

Akey feature ofthespatialfrequencydivision method is theuseofspatialfrequencyratherthandispersiontogenerateandseparateprobepulses.Notonlycanwavelength-sensitivemeasurements be avoided but pulse spectral information canalsoberetainedforfurtherspectroscopicanalysis.Thespatialcarrier frequency can be attached to the probe pulses throughеither interference or intensity modulation, as demonstratedusing the THPM and the FRAME techniques, respectively.The THPM technique can retrieve the amplitude and phaseinformation of ultrafast dynamics. The FRAME technique canbeeasilytransplantedintoexistingimagingsystems toachieve high-dimensional imaging of ultrafast events. How-ever, the poor sequence depth achieved with the frequencydivision method can only be increased by sacrificing eithertheFOVorspatialresolution.

The nine representative techniques based on the afore-mentionedfourmainmethodsaresummarizedintable1 in termsoftheirsystemlasersource,temporalresolution,framenumber, specifications, and applications to help researchersselectthemostsuitabletechniquefortheirspecificstudies.

3. Secondgenerationfour-dimensionalultrafastelectronmicroscopy

During femtosecond laser fabrication, photons are mainlyabsorbed by electrons, and the subsequent energy transferfrom electrons to ions

occurs over a time scale of picose-conds.Hence,femtosecondphoton-electroninteractionsdominate the whole fabrication process, which poses a chal-lenge in terms of measurement and control at the electronlevel during fabrication processes. Pump-probe and ultrafastcontinuousimagingtechniquesareviablesolutionscrucialforunderstanding phenomena such as electron relaxation, carrierdynamics, and charge transfer. Hence, the challenge lies incombiningtheatomicspatialresolutionoftheelectronmicroscope with the ultrafast temporal resolution of time-resolved spectroscopy to devise a unique analytical tool thatcanprovidedynamicinformationaboutmoleculareventswithextremely fine detail simultaneously in both space and time.The ability to access carrier dynamics selectively on materialsurfaces with high temporal and spatial control in a photo-induced reaction is a particularly challenging task that canonlybeachievedbyapplyingfour-dimensionalultrafast electron microscopy (4D UEM) with time-resolved imagesthathavenanometerspatialandfemtosecondtemporalreso-lutions. Although thereis a problem of contaminationofvacuum system by the laser ablated materials, the 4D UEMcanwellrealizetheobservationofvariousphenomenabeforelaser ablation. In addition, if the 4D system works in a singlepulse mode, the amount of ablated materials is small andcontrollable.Recently,asanew directionin4Delectronmicroscopy,secondgeneration ultrafastelectronmicroscopy (S-UEM),with650fsand5 nmtemporalandspatialresolutions,wasdevelopedforthevisualizationofmaterials dynamics[96–100].

Experimental setupofS-UEM

A description of the 4D S-UEM experimental design is givenin this section to help comprehend the manner in which themeasurementsarerealized[96].The4DS-UEMexperimentalsystemintegrateafemtosecondClark-MXRfiberlaserwithamodifiedFEIQuanta650scanningelectronmicroscope (figure 23). The 1030 nm, 270 fs laser pulse is divided by abeam splitter and directed toward two independent harmonicgenerators (HGs) to produce the second and third harmonicsignals,respectively.TheoutputofthefirstHG(343or515 nm) isdirectedwithprecisionthroughapyrometric quartz window and is focused tightly on a cooled Schottkyfield-emitter tip (zirconium-oxide-coated tungsten) to gen-eratethepulse,whereasthe515nmoutputisdirectedontothe sample as a pump pulse to photoexcite the specimen understudy. The relative timing between the two pulses is adjustedwithprecisionthroughacomputer-controlledopticaldelay

Table1.Comparativesummaryofrepresentativecontinuousultrafastopticalimagingtechniques.

Typicaltechnique	Laserpulse	Temporalresolution	Framenumber	Imageacquisition	Applications
M-FTOP[62]	65fs,800nm	0.96ps	4	Direct	Laserpulsecharacterization
STAMP[72]	70fs,810nm	229fs	6	Direct	Laserplasma;phonondynamics
SF-STAMP[74]	70fs,810nm	133fs	25	Direct	Laserinducedphasetransition
CUST[80]	50fs,800nm	260fs	60	Reconstruction	Laserpropagation
ADMC[81]	30fs,800nm	250fs	4	Direct	Laserplasma
OCFI[82]	10ps,527nm	34ps	4	Reconstruction	Laserplasmaandelectrondensity
SS-FDT[83]	30fs,800nm	2.5ps	5	Reconstruction	Highnonlinearopticalphysics
THPM[90]	30ps,1064nm	1.6ns	2	Reconstruction	Laser-induceddamage
FRAME[95]	125fs,800nm	200fs	4	Reconstruction	Laserpulsecharacterization

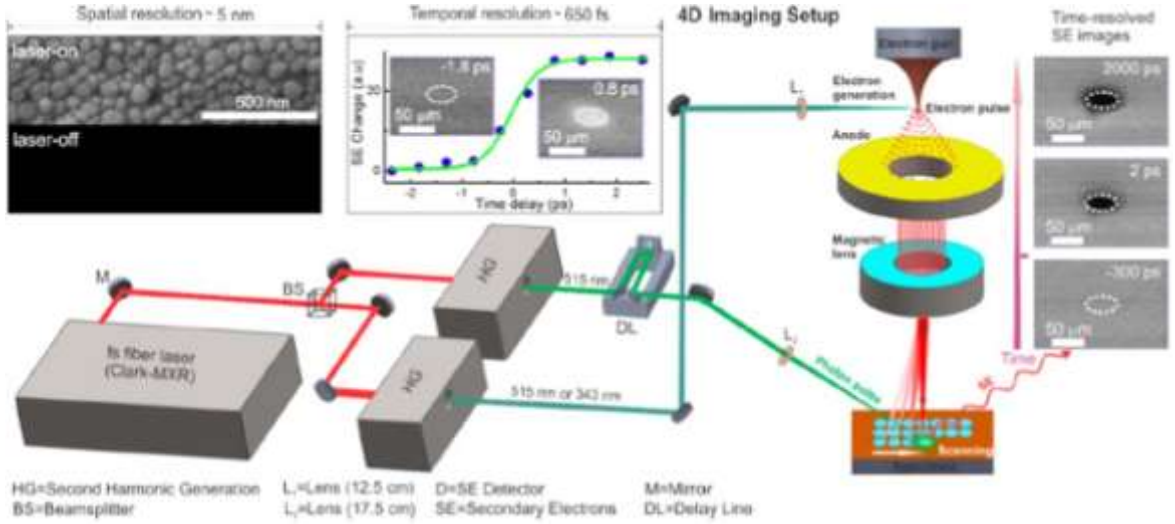

Figure23.SchematicoftheS-UEMexperimentalsetup.Reprintedwithpermissionfrom[96].Copyright(2016)AmericanChemicalSociety.

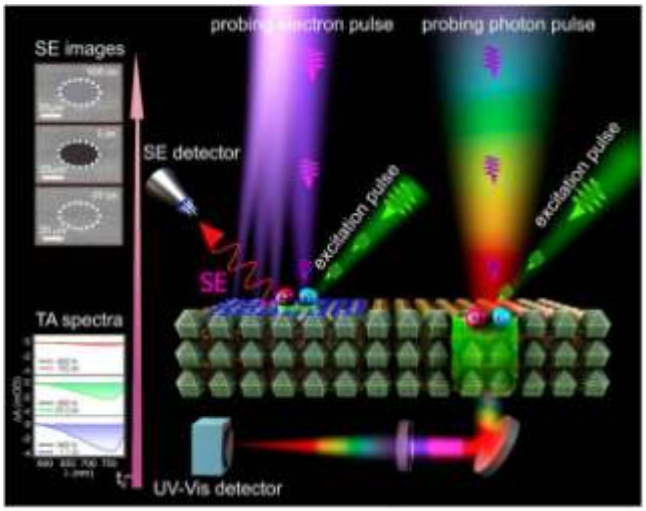

Figure24.MechanismsofthedynamicsobservedwiththeS-UEM,wherethevalencebandelectronsarepromotedtotheconductionbanduponopticalexcitation.Thedashedellipseindicatesthelocationofthelaseronthespecimen.Severaltime-resolvedimagesatselectedtimesaredisplayedtoindicatecontrastdevelopment.

Highcontrastisrecordedbecauseoftheenergygain,anddarkcontrastisrecordedbecauseoftheenergylossatthecenteroftheexcitedregion.Reprintedwithpermissionfrom[97].Copyright(2017)AmericanChemicalSociety.

line.ApositivelybiasedEverhart-Thornleydetectorisusedtocollect the secondary electrons (SEs) emitted from the specimen.Throughtheimagingofgoldnanoparticlesusing pulsed-generated photoelectrons, the spatial resolution of theS-UEMwasdeterminedtobeapproximately5 nm.Thetemporal resolution of 650 ± 100 fs was obtained by thekinetics plotted for the intensity change of the SEs from acadmiumselenide(CdSe)singlecrystal.

Mechanisms ofthe dynamicsobservedwiththe4DS-UEM

Onecandeterminetheregimeofdynamicprobingdependingonthetimedelaybetweentheclockingphotonpulseinitiatingthe sample dynamics and the photoelectron probing pulsegenerated through photoexcitation by using a field emission gun[97].Experimentally,acomputer-controlleddelaylinecovering thetimerangefrom−0.6to6.0nsisusedtodefinethetimeaxisoftheacquiredSEimages.ThedifferencesoftheSE

imagescanbeextractedbysubtractingthereferencedim ageatnegativetimeframe.Contrast-enhancedimagescanbeobtainedfrom the pump pulse irradiated and nonirradiated regions. Either'bright' or 'dark' contrast can be observed, depending on thecollectednumberofSEswithrespecttothereference image

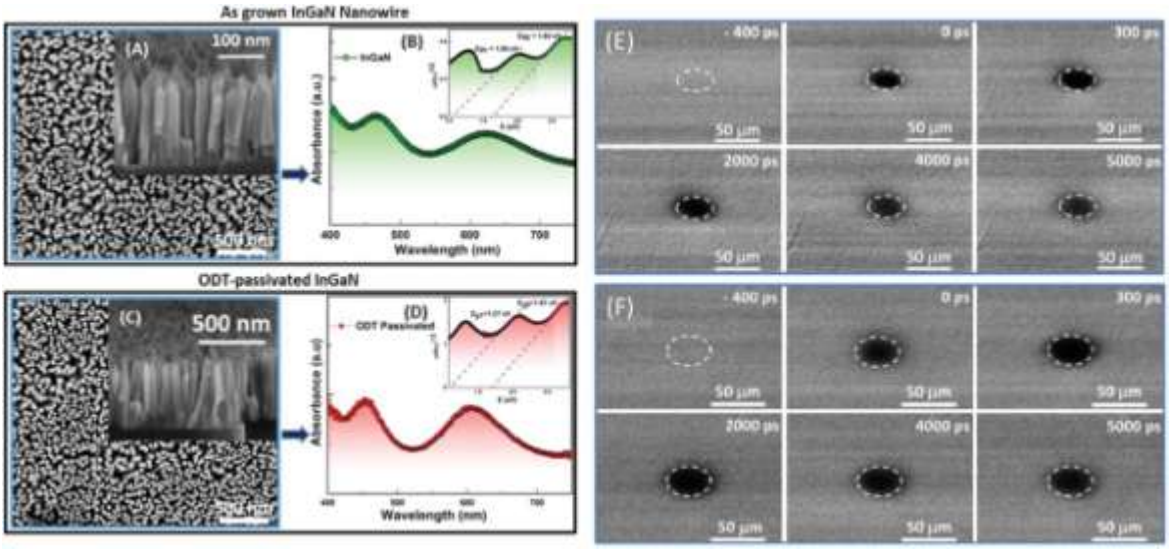

Figure 25.SEM images and steady-state measurements of the two samples. (a) SEM image of the surface of the as-grown NW films (cross-sectional image in the inset). (b) Absorption spectrum with the inset showing the Tauc plot. (c) SEM images of the ODT-passivated NWs(cross-sectionalimageintheinset).(d)AbsorptionspectrumwiththeTaucplotintheinset.Time-resolvedSEimagesofanInGaNNWarray (e)beforeand(f)aftersurfacepassivationwithODTattheindicatedtimedelays.[98]JohnWiley&Sons.©2016WILEY-VCHVerlag GmbH&Co.KGaA,Weinheim.

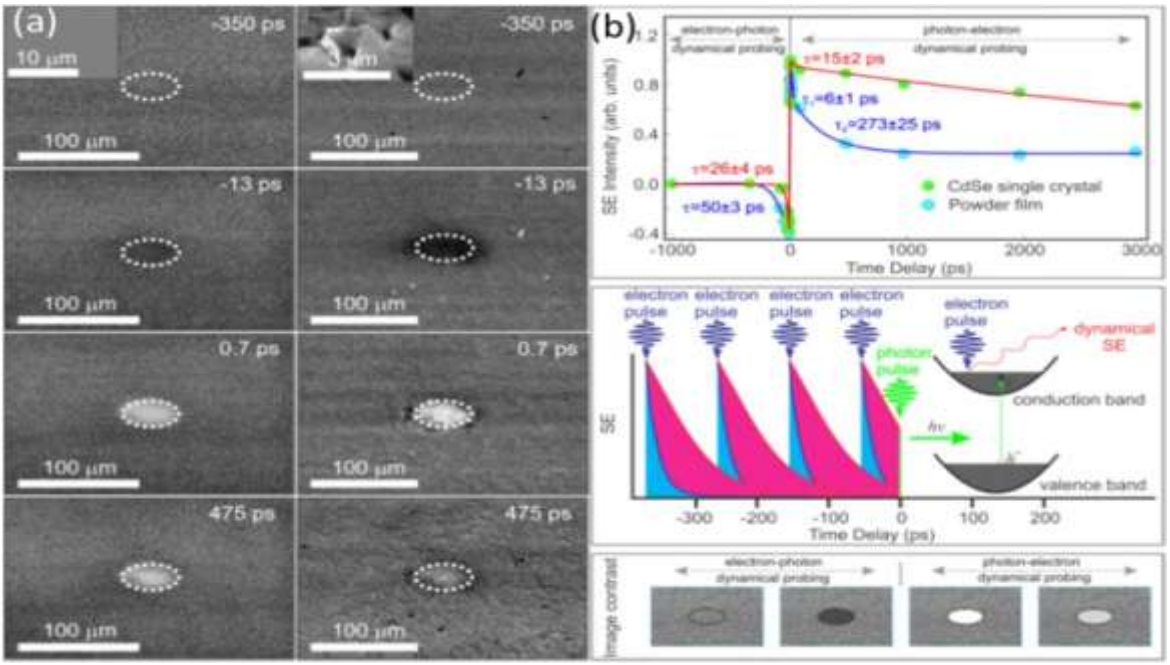

Figure26.(a)Time-resolvedSEimagesofasinglecrystal(left) andpowderfilm(right)ofCdSeattheindicatedtimedelays.TheSEMimages,whichexhibitthedistinguishablemorpholo

giesofthecrystalandthefilm,aredisplayedintheinsetsofthetwotopmostimages.
(b)DynamicsofthetemporalevolutionoftheSEintensityforbothsamples.Reprintedwithpermissionfrom[99].Copyright(2015)
AmericanChemicalSociety.

(figure24).Therearetwoprobingregimes.Acommonlyusedprobingregimeiscalledphoton-electrondynamicalprobing,inwhichaclockingopticalpulsearrivesbeforetheprobing electronpulse.Anotherprobingregimeiscalledelectron-
photon dynamical probing, which means that the electron pulsearrives before the clocking pulse. The two probing regimesconsiderablyinfluencethenatureoftheimagecontrastthatcanbeobtainedthroughsuchtime-resolvedmeasurements.

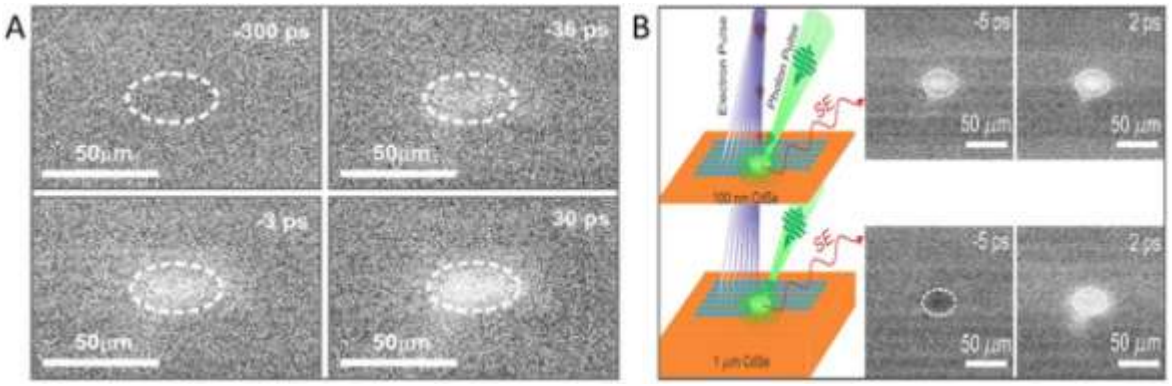

Figure 27.CdSe dynamics under different experimental conditions. (a) Time-resolved difference images of a CdSe (0001) single crystal inselected timeframes obtained withkeVpulsed primary electrons. (b) Time-resolved difference images of 100 nm and 1 µm thick CdSe filmsobtainedwith30keVpulsedprimaryelectrons.Reprintedwithpermissionfrom[100].Copyright(2017)American ChemicalSociety.

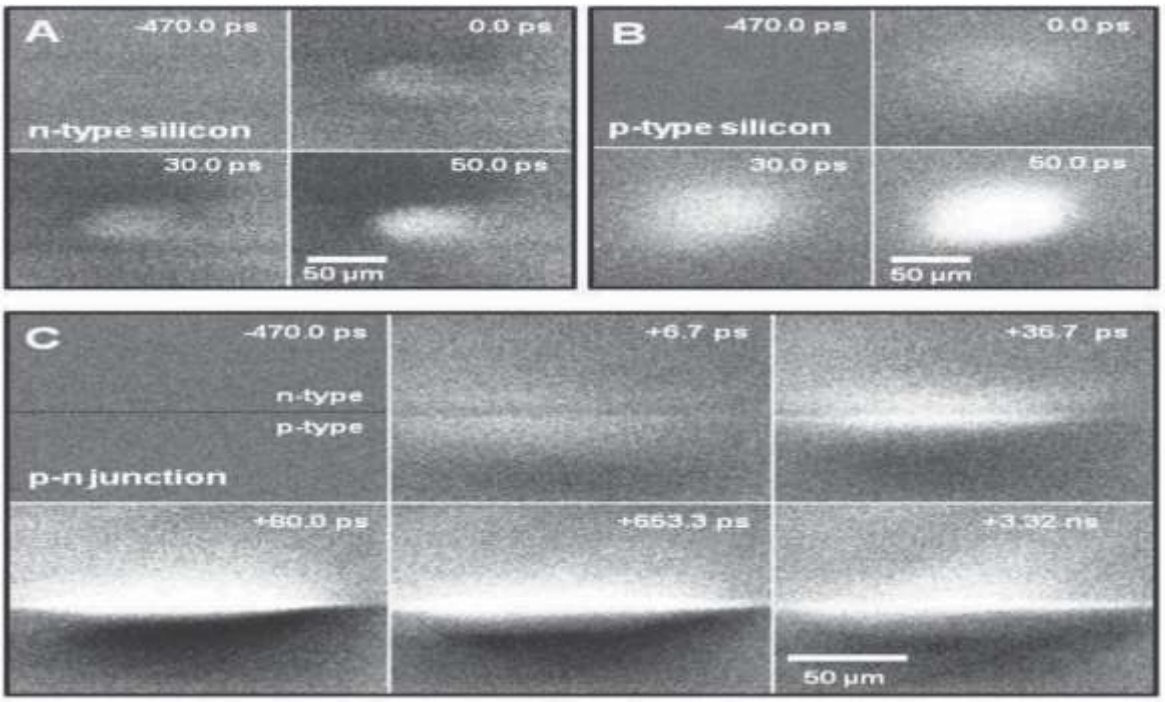

Figure 28.SE difference images at the indicated time delays for (a) n-type Si and (b) p-type Si. (c) SE difference images at the indicated timedelaysforaSip–njunction.Reproducedwithpermissionfrom[101].

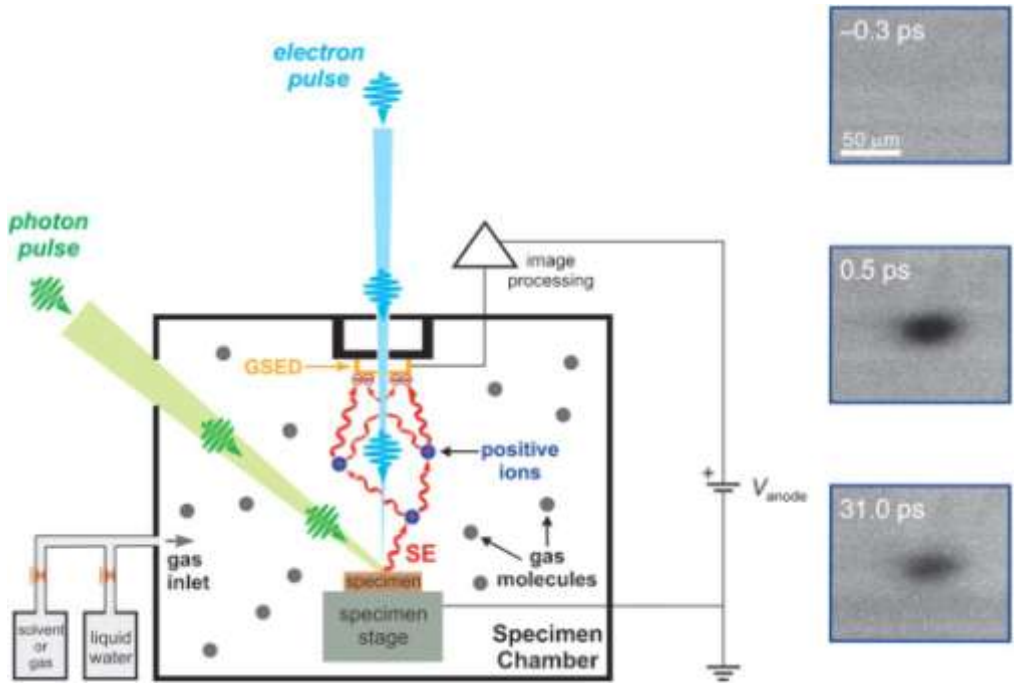

Figure 29.Environmental S-UEM (schematic) and three experimental frames at −0.3, 5.0, and 31.0 ps. The figure displays the two pulsesinvolved,primaryelectronprobe,andclockingopticalpulsethatinitiatesthechange.[102]JohnWiley&Sons.Copyright©2013WILEY-VCHVerlagGmbH&Co.KGaA,Weinheim.

Illustrativeexamples

Chargecarrierdynamicsonthesurfaceofindiumgallium nitride nanowires (NWs).An S-UEM was employedto image the charge carrier dynamics and carrier diffusion onthesurfaceof indiumgalliumnitride (InGaN)NWs[98].Thekinetics of the SE intensity evolution and time-resolved SEimagesindicatedthatcarrierrecombinationdecreasedconsiderablyfrom40%to15%onoctadecylthiol(ODT) treatmentwithintheobservedtimewindow(figure25), which provideddirectevidenceoftheremovalofsurfacestates and hencenonradiativecarrierrecombinationpathwaysinrealspaceandtime.

Effect of the morphology on the surface charge carrierdynamics.An S-UEM was used to determine the effect ofsurface morphology on surface charge carrier dynamics [99].IncontrasttoasinglecrystalofCdSe,rapidrecoveryofthe SE signal was observed in a CdSe powder film (figure 26).Thisdifferencecanbeascribedtothefactthatthesurface defectsinthepowderfilmcanserveasfastcarrier-quenchingcentersthatconsiderablyreducethenumberofexcitedcarriers, which results in bright contrast. This proves thatsurface morphologyiscrucialfordeterminingthe chargecarrierdynamicsofphotoactivematerials. Furthermore,thefundamentaleffectoftheabsorberlayerthickness on the charge carrier dynamics was studied [100].Time-resolved images indicate that the dynamics of chargecarriers were highly sensitive to the thickness of absorberlayer, as demonstrated using CdSefilms of different thicknessesasamodelsystem(figure27).Thisfinding providedthefoundationfortheapplicationofanS-UEMtoawiderangeofdevicesusedinmaterialsresearch,andaffectedtheoptimizationofphotoactivematerialsinthesedevices.

Chargecarriertransportatthep–njunction.AnS-UEMwasusedtostudychargecarriergeneration,transport,and recombinationat asilicon p–n junctionwithawell-definednanoscaleinterface[101].Contrarytothe expectedrangeofthetrusteddrift-diffusionmodel,theseparationofcarriersinthep−njunctionextendedconsiderablybeyondthedepletionlayer.Moreover,thecarrierdensitylocalizedacrossthejunctionoveratimerangeofuptotensofnanosecondsdependingonthelaser fluence (figure 28). The observations revealed a ballistic-typemotion and formed the basis of a model that accounts for thespatiotemporaldensitylocalizationacrossthejuncti

on.

Mapping surface solvation in space and time.Theultrafastobservationofsolvationdynamicswasrealizedbyan S-UEM in the environmental mode at 'wet' material surfacesbeyondthediffractionlimitofvisiblelight[102].Asprototypes for mapping surface solvation in space and time,CdSesurfaceswithatomicallydistinctsurfacestructuresand coatedwithpolarandnonpolarmoleculeswerestudied(figure 29). The distinct dynamic behaviors originated fromthedifferencesininteractionsandstructuresbetweenambient adsorbatemoleculesandthesurfacesinvolved.An S-UEMintheenvironmentalmodecanpotentiallybeused toexplore reactivity and interfacial phenomena with the temporal andspatialscalesofstructuraldynamics.

SUMMARY AND OUTLOOK

Insummary,thedevelopmentsinultrafastchemistryandultrafastphysicshavemadeitpossibletoobserveandcontrolelectron dynamics in manufacturing, which is expected toconsiderablypromotethedevelopmentofbasicmanufacturingresearch.Intheobservationofthelocalinstantaneouselectrondynamic spatiotemporal evolution process in ultrafast lasermanufacturing, the consideration of temporal and spatial resolutionsandpanoramicmeasurementatdifferentscalesaretwomajorchallenges.Toaddressthechallenges,wehavereviewedthe principles and applications of major ultrafast optical ima-gingmethods,such as thepump-probemethod,STAMP,CUST, THPM, FRAME, and 4D S-UEM. We have analyzedhow these methods circumvent the limitations of traditionalimage sensors to achieve increased frame rates and shutterspeeds.Althoughthemethodstradeoffoneormoreparametersofspecificityforanincreasedimage-acquisitionspeed,theyarecomplementary to each other. In the near future, a multiscaleobservation system with high spatial-temporal resolution anddynamic continuous observation capability could be establishedby combining pump detection, new ultrafast continuous ima-gingtechnology,andimproved4DS-UEMtechnology.Suchasystemcouldbeusedtodetermineevolution ofthestructure and properties from electron ionization (femtosecond-picose-cond scale) and material phase transition (picosecond–nano-secondscale) inamanufacturingactivityinwhichtheobservationsofmultiscaleprocesseshavehighspatial-temporal resolution, which would bring about a paradigm shift in fem-tosecondlasermanufacturing.withvaryingspotsizeOpt.Express2315608–15

REFERENCES

[1] GattassRandRandMazurE2008Femtosecondlasermicromachiningintransparentmaterials Nat.Photon.2219
[2] SugiokaKandChengY2014UltraCastlasersreliabletoolsforadvancedmaterialsprocessingLight:Sci.Appl.3149
[4] KerseC,Kalaycıoğlu H,ElahiP,ÇetinB,Kesim DK,AkçaalanÖandHolzwarthR2016Ablation-cooledmaterialremovalwithultrafastburstsofpulsesNature53784
[5] JiangLandTsaiHL2005RepeatablenanostructuresindielectricsbyfemtosecondlaserpulsetrainsAppl.Phys.Lett.87151104
[6] Zhao Y, Han Q, Cheng Z, Jiang L and Qu L 2017 Integratedgraphene systems by laser irradiation for advanced devicesNanoToday1214–30
[7] TanD,SharafudeenKN,YueYandQiuJ2016Femtosecondlaser induced phenomena in transparent solid materials:fundamentalsandapplicationsProg. MaterSci.76154–228
[8] YinK,DuanJA,SunX,WangCandLuoZ2015Formationofsuperwettingsurfacewithline-patternednanostructureonsapphireinducedbyfemtosecondlaserAppl.Phys.A11969–74
[9] WangC,LuoZ,DuanJA,JiangL,SunX,HuYandLuY2015 Adjustable annular rings of periodic surface structuresinducedbyspatiallyshapedfemtosecondlaserLaserPhys.Lett.12056001
[10] WangA,JiangL,Li X,LiuY,DongX,QuLandLuY 2015Mask- free patterning of high- conductivity metal nanowiresin open air by spatially modulated femtosecond laser pulsesAdv.Mater.276238–43
[11] FanP,BaiB,LongJ,JiangD,JinG,ZhangHandZhongM2015 Broadband high-performance infrared antireflectionnanowires facilely grown on ultrafast laser structured CusurfaceNanoLett.155988–94
[12] CaoYY,TakeyasuN,TanakaT,DuanXMandKawataS2009 3D metallic nanostructure fabrication by surfactant-assistedmultiphoton-inducedreductionSmall51144–8
[13] JiangL,WangAD,LiB,CuiTHandLuYF2018 Electronsdynamicscontrolbyshapingfemtosecondlaserpulsesinmicro/nanofabrication:modeling,method,measurementandapplicationLight:Sci.Appl.717134
[14] LiangJandWangLV2018Single-

shotultrafastopticalimagingOptica51113
[15] HebeisenCT,SciainiG,HarbM,ErnstorferR,Kruglik S G and Miller R J D 2008 Direct visualization ofcharge distributions during femtosecond laser ablation of aSi(100)surfacePhys.Rev.B78081403(R)
[16] HuH,LiuTandZhaiH2015Comparisonoffemtosecondlaser ablation of aluminum in water and in air by time-resolvedopticaldiagnosisOpt.Express23628–35
[17] HarilalSS,DiwakarPK,PolekMPandPhillips MC2015Morphologicalchangesinultrafastlaserablationplumes]AnoopKK,HarilalSS,PhilipR,BruzzeseRandAmorusoS2016 Laser fluence dependence on emission dynamics ofultrafast laser induced copper plasma J. Appl. Phys. 120185901
[18] ZhangN,ZhuX,YangJ,WangXandWangM2007Time-resolvedshadowgraphsofmaterialejectioninintensefemtosecondlaserablationofaluminumPhys.Rev.Lett.99167602
[19] HuH,WangX,ZhaiH,ZhangNandWangP2010 Generationofmultiplestresswavesinsilicaglassinhighfluencefemtosecond laser ablation Appl.Phys.Lett. 97 061117
[20] ZhaoXandShinYC2013Coulombexplosionandearlyplasmagenerationduringfemtosecondlaserablationofsiliconathighlaserfluence J.Phys. D:Appl.Phys.46335501
[21] KalupkaC, Finger J and Reininghaus M 2016 Time-resolvedinvestigations of the non-thermal ablation process of graphiteinducedbyfemtosecondlaserpulsesJ.Appl.Phys.119153105
[22] WangG,YuY,JiangL,LiX,XieQandLuY2017 Cylindrical Shockwave-induced compression mechanism infemtosecondlaserbesselpulsemicro-drillingofPMMAAppl.Phys.Lett.110161907